SUPPLEMENTARY INFORMATION

Metabolomics annotates ABHD3 as a physiologic regulator of medium-chain phospholipids

Jonathan Z. Long, Justin S. Ciar, David Milliken, Sherry Niessen, Chu Wang, Sunia A. Trauger, Gary Siuzdak, Benjamin F. Cravatt

SUPPLEMENTARY METHODS

Materials. Pentadecanoic acid, C13 LPC, C14 LPC, C18 LPC, lysoPAF, PAF, C13/13 PC, C14/14 PC, C15/15 PC, C14/14 PE, C14/14 PA, C14/14 PS, C16/20:4 PC, C17:1 LPG, and C14/14-PG were purchased from Avanti Polar Lipids. oxPCs were purchased from Avanti Polar Lipids or Cayman Chemical. Arachidonic acid and linoleic acid were purchased from Sigma-Aldrich. d_4-palmitic acid was purchased from C/D/N Isotopes. FP-rhodamine was synthesized as described previously.[1,2] C18/2-PC was synthesized as described previously.[3] The synthesis of other C14-PCs is described below.

General synthetic methods. Unless otherwise noted, chemicals were obtained from commercial suppliers and used without further purification. Dry CH_2Cl_2 was obtained by passing commercially available pre-dried, oxygen-free formulations through activated alumina columns. NMR spectra were obtained in $CDCl_3$ and were recorded on a Bruker DRX-600 instrument equipped with a 5mm DCH cryoprobe. NMR chemical shifts are reported in ppm downfield relative to the internal solvent peak, and *J* values are in Hz. High resolution mass spectrometry data (HRMS) were performed at The Scripps Research Institute Mass Spectrometry Core and recorded on an Agilent mass spectrometer using ESI-TOF (electrospray ionization-time of flight).

General procedure for the synthesis of C14 PC lipids. To a solution of 0.1 M fatty acid (2.0 equiv) in dichloromethane was added *N,N*-dicyclohexylcarbodiimide (2.6 equiv) and *N,N*-dimethyl-4-aminopyridine (4.0 equiv). The solution was stirred at rt for 5 min. 1-myristoyl-2-hydroxy-*sn*-glycero-3-phosphocholine or 1-stearoyl-2-hydroxy-*sn*-glycero-3-phosphochline (1.3

equiv) was then added and the reaction was stirred for 24 h. Methanol was added (3 volume equivalents) and the mixture was incubated with Amberlight IR-120(plus) ion-exchange resin (800 mg) for 30 min. The solution was collected and beads washed with 5 ml MeOH. The combined filtrates were concentrated using rotary evaporation. Purification by silica flash chromatography (35:14:1 CH_2Cl_2:MeOH:H_2O) yielded PC species.

C14/16-PC, (*R*)-2-(7,7,8,8-d_4-palmitoyloxy)-3-(tetradecanoyloxy)propyl (2-(trimethylammonio)ethyl) phosphate. C14/d_4-16-PC obtained from d_4-7,7,8,8-palmitic acid in 23% yield (10.9mg, 0.023 mmol). ^{1}H-NMR (600 MHz, $CDCl_3$): δ 5.18 (m, 1H), 4.38 (d, *J* = 10.1 Hz, 1H), 4.30 (s, 2H), 4.11 (dd, *J* = 11.9, 7.6 Hz, 1H), 3.93-3.90 (m, 2H), 3.79 (s, 2H), 3.33 (s, 9H), 2.28 (dt, *J* = 15.4, 7.7 Hz, 4H), 1.61-1.55 (m, 4H), 1.30-1.25 (m, 42H), 0.87 (t, *J* = 7.0 Hz, 6H). ^{13}C-NMR (151 MHz, $CDCl_3$): δ 173.71, 173.39, 70.56, 66.41, 63.65, 63.12, 59.51, 54.51, 34.47, 34.28, 32.08, 29.89, 29.86, 29.75, 29.66, 29.54, 29.36, 25.15, 25.05, 22.85, 22.85, 14.28. HRMS (ESI) calcd for $C_{38}H_{72}D_4NO_8P$, *m/z* 710.5628 ($M+H^+$); found, *m/z* 710.5623.

C14/18:2-PC, (*R*)-2-((9*Z*,12*Z*)-octadeca-9,12-dienoyloxy)-3-(tetradecanoyloxy)propyl (2-(trimethylammonio)ethyl) phosphate. C14/18:2-PC obtained from lineolic acid in 55% yield (81.5 mg, 0.110 mmol). ^{1}H-NMR (600 MHz, $CDCl_3$): δ 5.38-5.28 (m, 4H), 5.17 (m, 1H), 4.37 (dd, *J* = 12.0, 2.7 Hz, 1H), 4.27 (s, 2H), 4.09 (dd, *J* = 12.0, 7.3 Hz, 1H), 3.90 (m, 2H), 3.78 (s, 2H), 3.34 (s, 9H), 2.74 (t, *J* = 6.9 Hz, 2H), 2.26 (m, 4H), 2.02 (m, 4H), 1.55 (m, 4H), 1.34-1.23 (m, 34H), 0.86 (m, 6H). ^{13}C-NMR (151 MHz, $CDCl_3$): δ 174.39, 173.98, 131.06, 130.80, 128.90, 128.70, 71.33, 67.11, 64.17, 63.84, 60.18, 60.15, 55.18, 35.15, 34.97, 32.77, 32.36, 30.55, 30.52, 30.40, 30.20, 30.14, 30.05, 29.97, 28.07, 28.04, 26.47, 25.80, 25.74, 23.54, 23.42, 14.98, 14.93. HRMS (ESI) calcd for $C_{40}H_{76}NO_8P$, *m/z* 730.5381 ($M+H^+$); found, *m/z* 730.5372.

C14/22:6-PC, (*S*)-2-((4*Z*,7*Z*,10*Z*,13*Z*,16*Z*,19*Z*)-docosa-4,7,10,13,16,19-hexaenoyloxy)-3-(tetradecanoyloxy)propyl (2-(trimethylammonio)ethyl) phosphate. C14/22:6-PC obtained from docosahexaenoic acid in 23% yield (18.2 mg, 0.023 mmol).[1]H-NMR (600 MHz, $CDCl_3$): δ 5.40-5.31 (m, 12H), 5.20 (s, 1H), 4.40-4.38 (m, 1H), 4.31 (s, 2H), 4.12 (dd, *J* = 12.0, 7.3 Hz, 1H), 3.97-3.90 (m, 2H), 3.80 (s, 2H), 3.35 (s, 9H), 2.84-2.80 (m, 10H), 2.37-2.34 (m, 4H), 2.27 (t, *J* = 7.6 Hz, 2H), 2.07 (m, 2H), 1.57-1.55 (m, 2H), 1.29 (s, 20H), 0.97 (t, *J* = 7.5 Hz, 3H), 0.87 (t, *J* = 7.0 Hz, 3H). [13]C-NMR (151 MHz, $CDCl_3$): δ 173.74, 172.67, 132.17, 129.46, 128.72, 128.50, 128.43, 128.20, 128.12, 127.99, 127.92, 127.13, 70.86, 70.82, 66.54, 66.50, 63.58, 63.55, 63.07, 59.49, 59.47, 54.59, 34.26, 32.08, 29.84, 29.71, 29.52, 29.49, 29.34, 25.68, 25.03, 22.85, 22.74, 20.71, 14.44, 14.27. HRMS (ESI) calcd for $C_{44}H_{76}NO_8P$, *m/z* 778.5381 ($M+H^+$); found, *m/z* 778.5370.

C14/20:4-PC, (*R*)-2-((5*E*,8*E*,11*E*,14*E*)-icosa-5,8,11,14-tetraenoyloxy)-3-(tetradecanoyloxy)propyl (2-(trimethylammonio)ethyl) phosphate. C14/20:4-PC obtained from arachidonic acid in 34% yield (18.2 mg, 0.034 mmol). **[1]H-NMR** (600 MHz, $CDCl_3$): δ 5.40-5.31 (m, 8H), 5.19 (m, 1H), 4.39 (dd, *J* = 11.9, 2.3 Hz, 1H), 4.30 (s, 2H), 4.11 (dd, *J* = 12.0, 7.3 Hz, 1H), 3.95-3.89 (m, 2H), 3.80 (s, 2H), 3.36 (s, 9H), 2.81 (m, 6H), 2.28 (m, 4H), 2.07 (m, 4H), 1.67 (m, 2H), 1.56 (m, 2H), 1.36-1.27 (m, 26H), 0.87 (m, 6H). **[13]C-NMR** (151 MHz, $CDCl_3$): δ 174.43, 173.81, 131.35, 129.77, 129.68, 129.48, 129.16, 128.93, 128.66, 128.35, 71.51, 67.23, 67.20, 64.22, 63.85, 60.16, 55.27, 34.97, 34.61, 32.78, 32.37, 30.58, 30.53, 30.41, 30.23, 30.19, 30.05, 28.07, 27.37, 26.48, 25.74, 25.71, 23.55, 23.43, 14.99, 14.95. **HRMS** (ESI) calcd for $C_{42}H_{76}NO_8P$, *m/z* 754.5381 ($M+H^+$); found, *m/z* 754.5377.

calcd for $C_{42}H_{76}NO_8P$, *m/z* 754.5381 ($M+H^+$); found, *m/z* 754.5377.

C18/16-PC, 2-(palmitoyloxy)-3-(stearoyloxy)propyl (2-(trimethylammonio)ethyl) phosphate. C18/16-PC obtained from palmitic acid in 20% yield (15 mg, 0.020 mmol). **^{1}H-NMR** (600 MHz, $CDCl_3$): δ 5.20 (s, 1H), 4.40-4.33 (m, 3H), 4.12 (s, 1H), 3.94 (s, 2H), 3.84 (s, 2H), 3.37 (s, 9H), 2.28 (dd, *J* = 19.1, 11.2 Hz, 4H), 1.57 (s, 4H), 1.25 (s, 54H), 0.88 (t, *J* = 6.8 Hz, 6H). **^{13}C-NMR** (151 MHz, $CDCl_3$): δ 174.46, 174.16, 72.06, 67.21, 64.38, 63.86, 60.31, 60.20, 55.28, 35.20, 35.01, 32.81, 31.81, 30.64, 30.57, 30.55, 30.51, 30.33, 30.29, 30.26, 30.13, 30.08, 23.57, 14.99. **HRMS** (ESI) calcd for $C_{42}H_{84}NO_8P$, *m/z* 762.6007 ($M+H^+$); found, *m/z* 762.6008 .

C18/14-PC , (*R*)-3-(stearoyloxy)-2-(tetradecanoyloxy)propyl (2-(trimethylammonio)ethyl) phosphate. C18/14-PC obtained from palmitic acid in 47% yield (20 mg, 0.027 mmol). **^{1}H-NMR** (600 MHz, $CDCl_3$): δ 5.19 (s, 1H), 4.39-4.29 (m, 3H), 4.13 (s, 1H), 3.90 (s, 2H), 3.76 (s, 2H), 3.33 (s, 9H), 2.28 (dt, *J* = 14.1, 7.1 Hz, 4H), 1.57 (s, 4H), 1.25 (s, 50H), 0.87 (t, *J* = 6.8 Hz, 6H). **^{13}C-NMR** (151 MHz, $CDCl_3$): δ 174.44, 174.10, 71.34, 71.31, 67.21, 67.18, 64.34, 64.32, 64.30, 63.85, 60.24, 60.20, 60.18, 55.26, 35.20, 35.01, 32.80, 30.62, 30.60, 30.57, 30.55, 30.48, 30.28, 30.26, 30.25, 30.10, 30.05, 25.86, 25.78, 23.57, 15.00. **HRMS** (ESI) calcd for $C_{40}H_{80}NO_8P$, *m/z* 734.5694 ($M+H^+$); found, *m/z* 734.5683.

C18/12-PC,(*R*)-2-(dodecanoyloxy)-3-(stearoyloxy)propyl (2-(trimethylammonio)ethyl) phosphate. C18/12-PC obtained from palmitic acid in 49% yield (20 mg, 0.028 mmol). **^{1}H-NMR** (600 MHz, $CDCl_3$): δ 5.19 (s, 1H), 4.39-4.30 (m, 3H), 4.12 (s, 1H), 3.94 (s, 2H), 3.79 (s, 2H), 3.35 (s, 9H), 2.28 (dt, *J* = 12.8, 6.8 Hz, 4H), 1.56 (s, 4H), 1.25 (s, 46H), 0.87 (t, *J* = 6.8 Hz, 7H). **^{13}C-NMR** (151 MHz, $CDCl_3$): δ 174.43, 174.08, 71.40, 71.37, 67.24, 64.26, 63.86, 60.19, 60.17, 55.30, 35.20, 35.01, 32.80, 30.60, 30.56, 30.53, 30.44, 30.43, 30.24, 30.08, 30.03, 25.85,

25.77, 23.57, 15.00. **HRMS** (ESI) calcd for $C_{38}H_{76}NO_8P$, *m/z* 706.5381 ($M+H^+$); found, *m/z* 706.5372.

C18/10-PC, (*R*)-2-(decanoyloxy)-3-(stearoyloxy)propyl (2-(trimethylammonio)ethyl) phosphate. C18/10-PC obtained from palmitic acid in 60% yield (20 mg, 0.030 mmol). **^{1}H-NMR** (600 MHz, CDCl3): δ 5.19 (s, 1H), 4.39-4.30 (m, 3H), 4.13-4.10 (m, 1H), 3.93 (s, 2H), 3.77 (s, 2H), 3.32 (s, 8H), 2.28 (dt, *J* = 15.3, 7.6 Hz, 4H), 1.56 (s, 4H), 1.25 (s, 42H), 0.87 (t, *J* = 6.8 Hz, 6H). **^{13}C-NMR** (151 MHz, $CDCl_3$): δ 174.45, 174.12, 71.32, 71.28, 67.22, 67.18, 64.36, 63.83, 60.23, 60.21, 55.26, 35.18, 35.00, 32.80, 32.77, 30.61, 30.59, 30.54, 30.47, 30.38, 30.25, 30.24, 30.21, 30.10, 30.03, 25.84, 25.77, 23.56, 14.99, 0.87. **HRMS** (ESI) calcd for $C_{36}H_{72}NO_8P$, *m/z* 678.5068 ($M+H^+$); found, *m/z* 678.5068.

C18/8-PC, (*R*)-2-(octanoyloxy)-3-(stearoyloxy)propyl (2-(trimethylammonio)ethyl) phosphate. C18/8-PC obtained from palmitic acid in 26% yield (10 mg, 0.015 mmol). **^{1}H-NMR** (600 MHz, $CDCl_3$): δ 5.19 (s, 1H), 4.39-4.32 (m, 3H), 4.13-4.10 (m, 1H), 3.94-3.91 (m, 2H), 3.81 (d, *J* = 0.5 Hz, 2H), 3.42-3.28 (m, 9H), 2.28 (dd, *J* = 15.6, 7.7 Hz, 4H), 1.57 (d, *J* = 5.7 Hz, 4H), 1.37-1.18 (m, 40H), 0.90-0.83 (m, 7H). **^{13}C-NMR** (151 MHz, $CDCl_3$): δ 174.47, 174.13, 71.36, 67.31, 67.29, 64.36, 63.87, 60.18, 60.15, 55.37, 35.19, 35.00, 32.80, 32.57, 30.59, 30.57, 30.54, 30.44, 30.24, 30.08, 29.94, 29.87, 25.83, 25.77, 23.57, 23.50, 15.00, 14.96, 0.87. **HRMS** (ESI) calcd for $C_{34}H_{68}NO_8P$, *m/z* 650.4755 ($M+H^+$); found, *m/z* 650.4750.

C18/C9-PC, (*R*)-2-(nonanoyloxy)-3-(stearoyloxy)propyl (2-(trimethylammonio)ethyl) phosphate. C18/9-PC obtained from palmitic acid in 40% yield (15 mg, 0.023 mmol). **^{1}H-NMR** (600 MHz, $CDCl_3$): δ 5.18 (s, 1H), 4.38-4.30 (m, 3H), 4.11 (s, 1H), 3.92 (s, 2H), 3.76 (s, 2H), 3.32 (s, 9H), 2.27 (dt, *J* = 15.4, 7.5 Hz, 4H), 1.56 (s, 4H), 1.24 (s, 40H), 0.87 (t, *J* = 6.6 Hz, 6H). **^{13}C-NMR** (151 MHz, $CDCl_3$): δ 174.46, 174.14, 71.33, 67.23, 64.42, 63.85, 60.23, 55.27, 35.18,

35.00, 32.80, 32.73, 30.60, 30.59, 30.54, 30.46, 30.24, 30.19, 30.09, 30.07, 30.01, 25.83, 25.77, 23.57, 23.53, 15.00, 14.98. **HRMS** (ESI) calcd for $C_{35}H_{70}NO_8P$, *m/z* 664.4912 ($M+H^+$); found, *m/z* 664.4922.

C18/C6-PC, (*R*)-2-(hexanoyloxy)-3-(stearoyloxy)propyl (2-(trimethylammonio)ethyl) phosphate. C18/6-PC obtained from palmitic acid in 42% yield (15 mg, 0.024 mmol). **^{1}H-NMR** (600 MHz, $CDCl_3$): δ 5.19 (s, 1H), 4.33 (d, *J* = 46.1 Hz, 3H), 4.12 (s, 1H), 3.92 (s, 2H), 3.76 (s, 2H), 3.33 (s, 9H), 2.27 (dd, *J* = 15.5, 7.5 Hz, 4H), 1.57 (s, 4H), 1.25 (s, 32H), 0.87 (t, *J* = 7.2 Hz, 6H). **^{13}C-NMR** (151 MHz, $CDCl_3$): δ 174.45, 174.11, 71.38, 71.35, 71.34, 67.23, 67.18, 64.36, 63.85, 60.21, 55.26, 35.12, 35.00, 32.79, 32.09, 30.59, 30.57, 30.54, 30.44, 30.24, 30.23, 30.07, 25.76, 25.47, 23.19, 15.00, 14.81. **HRMS** (ESI) calcd for $C_{32}H_{64}NO_8P$, *m/z* 622.4469 ($M+H^+$); found, *m/z* 622.4457.

C18/C5-PC, (*R*)-2-(pentanoyloxy)-3-(stearoyloxy)propyl (2-(trimethylammonio)ethyl) phosphate. C18/5-PC obtained from palmitic acid in 44% yield (15 mg, 0.025 mmol). **^{1}H-NMR** (600 MHz, $CDCl_3$): δ 5.19 (s, 1H), 4.38-4.29 (m, 3H), 4.12 (s, 1H), 3.93 (s, 2H), 3.76 (s, 2H), 3.32 (s, 9H), 2.29 (dt, *J* = 24.0, 7.4 Hz, 4H), 1.57 (s, 4H), 1.25 (s, 32H), 0.89 (dt, *J* = 15.4, 7.5 Hz, 6H). **^{13}C-NMR** (151 MHz, $CDCl_3$): δ 174.47, 174.16, 71.39, 71.34, 68.68, 67.21, 67.18, 64.40, 64.37, 60.21, 55.22, 34.99, 34.86, 32.80, 30.59, 30.57, 30.54, 30.44, 30.24, 30.08, 27.84, 25.76, 23.56, 23.04, 15.00, 14.62. **HRMS** (ESI) calcd for $C_{31}H_{62}NO_8P$, *m/z* 608.4213 ($M+H^+$); found, *m/z* 608.4294.

Cell transfection and untargeted metabolomics measurements. Full-length cDNAs encoding serine hydrolases have been previously reported[4]. HEK293T cells were grown to ~70% confluence in 10 cm dishes in complete medium (DMEM with L-glutamine and FCS) at 37°C

and 5% CO_2. The cells were transiently transfected by using the appropriate cDNA (5 µg) or empty vector control ("mock") and the FUGENE 6 (Roche Applied Science) transfection reagents following the manufacturers' protocols. After 24 h, cells were trypsinized and replated in triplicate at 2 million cells/well in 6-well dishes. After an additional 24 h, the media was aspirated, the cells were washed once with PBS, and incubated with 1 ml serum free media (DMEM with L-glutamine). After 1 h serum starvation, the media was aspirated and the cells were collected in 1 ml 50 mM Tris pH 8. Lipids from this cell suspension were directly extracted in an additional 3 ml of 2:1 v/v chloroform/methanol. The mixture was vortexed and then centrifuged (1,400 x *g*, 10 min). The organic layer was removed, dried under a stream of N_2, resolubilized in 2:1 v/v $CHCl_3$:MeOH (120 µl), and 30 µl of this resolubilized lipid was injected onto an Agilent 1100 series LC-MSD SL instrument. LC separation was achieved with a Gemini reverse-phase C18 column (5 µm, 4.6 mm x 50 mm, Phenomonex) together with a pre-column (C18, 3.5 µm, 2 mm x 20 mm). Mobile phase A was composed of 95:5 v/v H_2O:MeOH, and mobile phase B was composed of 60:35:5 v/v/v *i*-PrOH:MeOH:H_2O. 0.1% ammonium hydroxide and 0.1% formic acid was included to assist in ion formation in negative and positive ionization mode, respectively. The flow rate was 0.5 ml/min and the gradient consisted of 5 min 0% B, a linear increase to 100% B over 15 min, followed by an isocratic gradient of 100% B for 12 min before equilibrating for 5 min at 0% B (37 min total). MS analysis, in scanning mode from scanning from m/z = 200–1200, was performed with an electrospray ionization (ESI) source. The capillary voltage was set to 3.0 kV and the fragmentor voltage was set to 100 V. The drying gas temperature was 350°C, the drying gas flow rate was 10 l/min, and the nebulizer pressure was 35 psi. The chromatograms were analyzed as described below.

Analysis of chromatograms from cellular metabolomes. In order to identify candidate metabolites that show distinct levels of abundance in different enzyme transfections, a utility software "makePlotJZL" was developed in the R programming language. The program uses the XCMS library[5] to read in raw MS data in either CDF or XML format and generates averaged ion intensities at unit *m/z* intervals from the mock and enzyme-transfected samples. For each unit *m/z* interval, a single PDF page containing multiple plots is generated. Each plot is a comparison of extracted ion chromatograms between a given enzyme (shown in red) and mock (shown in black). Because each PDF page contains multiple plots each corresponding to a different enzyme, visual inspection of these PDF pages allows for the rapid identification of large changes in highly abundant ions selective to one enzyme transfection but not others. After exclusion of metabolites that were changed in multiple enzyme transfections, we identified and verified two selective hits (*m/z* = 524 for ABHD3, and *m/z* = 391 for CES2, see **Fig. 1a** and **Supplementary Fig. 3**) from our initial screen of 12 enzymes. The software, with instructions for its use, is publicly accessible at the following URL:
http://www.scripps.edu/chemphys/cravatt/makePlotJZL/

Tandem MS fragmentation experiments. MS/MS analysis was performed on an Agilent 6520 series quadrupole-time of flight (Q-TOF) instrument, using the same LC separation and buffers as described above for positive ionization mode. MS and MS/MS data collection, both in scanning mode from *m/z* = 50–800 and a rate of 1.02 spectra/s, was performed with an electrospray ionization (ESI) source. The capillary voltage was set to 4.0 kV and the fragmentor voltage was set to 100 V. The drying gas temperature was 350°C, the drying gas flow rate was

11 l/min, and the nebulizer pressure was 45 psi. The collision energy for all LPC and PC metabolites was 30 V.

Generation of stable epitope-tagged ABHD3, ABHD3-S220A, and GFP cell lines. The catalytic serine of mouse ABHD3 was mutated to Ala (S220A) using the QuikChange II site-directed mutagenesis kit, according to manufacturer's protocol, and the following primers: sense, CTGGCAGCAGGCGTAGCAATGGGAGGAATGC, antisense, GCATTCCTCCCATTGCTACGCCTGCTGCCAG. These constructs were tagged with myc-His epitopes at the C-terminus and cloned into pCLHCX vector (Imgenex) to generate stable cell lines as described previously[6].

Preparation of mouse tissue and cell line proteomes. Mouse brains were Dounce-homogenized in PBS, pH 7.5, followed by a low-speed spin (1,400 x *g*, 5 min) to remove debris. The supernatant was then subjected to centrifugation (64,000 x *g*, 45 min) to provide the membrane fraction as a pellet. The pellet was washed and resuspended in PBS buffer by sonication. Total lysates was harvested from cell lines by washing cells with PBS and then mechanical scraping. The cell pellets were isolated by centrifugation (1,400 x *g*, 5 min), resuspended in PBS by sonication. Total protein concentration in each fraction was determined using a protein assay kit (Bio-Rad). Samples were stored at –80°C until use.

FP-Rh labeling of tissue and cell line protomes. Tissue or cell line proteomes were diluted to 1 mg/ml in PBS and FP-Rh[1] was added at a final concentration of 1 μM in a 50 μl total reaction volume. After 30 min at 25°C, the reactions were quenched with 4x SDS-PAGE loading buffer,

boiled for 5 min at 90°C, subjected to SDS-PAGE and visualized in-gel using a flatbed fluorescence scanner (Hitachi).

Assay for phospholipase activity. Total cell lysate proteome (30 μg) from C8161 cells overexpressing epitope-tagged ABHD3 or ABHD3-S220A was suspended in PBS pH 7.5 (100 μl) and substrates (100 μM final), as 10 mM stock solutions in ethanol (PCs) or DMSO (all other lipids), were added for 1% final ethanol or DMSO. The reactions were incubated at 37°C for 1 h and quenched by the addition of 300 μl 2:1 v/v chloroform/methanol with 1 nmol internal standard (the appropriate lysophospholipid or free fatty acid product). A portion of the organic phase (20 μl) was injected onto an Agilent 1100 series LC-MSD SL instrument. LC separation and MS parameters was identical to those described above. Hydrolysis products were quantified by measuring the area under the peak in comparison to the internal standard.

***Abhd3*$^{-/-}$ mice.** *Abhd3*$^{-/-}$ mice, obtained by homologous recombination, were purchased from Deltagen. The endogenous and targeted *Abhd3* alleles were amplified by PCR of genomic tail DNA using the following primers: GGAAGTGATGAAGGGTCTCAGCAATGTC and GACACTGCTAAGTCCACTAGTTGCTGG (endogenous); GGAAGTGATGAAGGGTCTCAGCAATGTC and CAAATTAAGGGCCAGCTCATTCCTCC (targeted), to give bands of size 226 bp (endogenous) or 373 bp (targeted). PCR conditions were as follows: 95 °C 5 min, then 50 cycles of 95 °C 30 s, 55 °C 30 s, and 72 °C 30 s, then 72 °C 5 min, with 400 nM of each primer and 2 μl of genomic DNA. Animal experiments were conducted in accordance with the guidelines of the Institutional Animal Care and Use Committee of The Scripps Research Institute.

Untargeted MS-based proteomics of brain membranes proteome from *Abhd3*$^{-/-}$ mice. 200 μg of brain membrane proteins were TCA precipitated. 100 μg of TCA precipitated proteins were resuspended in 8M urea in 50 mM Tris pH 8.0 and digested with trypsin in the presence of PROTEASMAX (Promega) according to manufacturer's protocol. Peptides were acidified to a final concentration of 5% formic acid and spun at 17,000 x g for 30 minutes. The supernatant were loaded onto a biphasic (strong cation exchange/reverse phase) capillary column for multidimensional protein identification analysis (MudPIT) in combination with a single reverse phase tip. Peptides were separated and analyzed by 2D-LC separation in combination with tandem MS as previously described using an 11 step gradient[7]. Data-dependent tandem mass spectrometry (MS/MS) analysis was performed using a Velos-Orbitrap hybrid mass spectrometer (Thermo Scientific). Full MS spectra were acquired in profile mode, with a mass range of 400–1800 in the Orbitrap analyzer with resolution set at 30,000 followed by 30 MS/MS scans in the ion trap. Dynamic exclusion was enabled with a repeat count of 1, a repeat duration of 20 s, exclusion duration 20s and an exclusion list size of 300. All tandem mass spectra were collected using a normalized collision energy of 35%, an isolation window of 2 Da and an activation time of 10 ms. One micro scan was applied for all experiments in Orbitrap or LTQ. Spray voltage was set to 2.50 kV and the flow rate through the column was 0.20 μl/min.

RAW files were generated from mass spectra using XCalibur and MS/MS spectra data extracted using RAW Xtractor (version 1.9.1) which is publicly available (http://fields.scripps.edu/?q=content/download). MS/MS spectral data were searched using the PROLUCID algorithm against a custom made database containing 23,421 mouse IPI sequences that were concatenated to a decoy database in which the sequences for each entry in the original

database was reversed[8]. In total the search database contained 46,842 protein sequence entries (23,421 real sequences and 23,421 decoy sequences). PROLUCID searches allowed for oxidation of methionine residues (15.99491 Da), static modification of cysteine residues (57.02146 Da-due to alkylation) and no enzyme specificity. As the peak selected for MS/MS analysis by the instrument control software is often not the monoisotopic ion, the search algorithm considers multiple isotopes, with a 50 ppm mass tolerance for each possible theoretical isotope peak. The validity of peptide/spectrum matches was assessed using DTASelect2 (version 2.0.27) and three defined parameters, the crosscorrelation score (XCorr), normalized difference in crosscorrelation scores (DeltaCN) and DeltaMass. DeltaMass is the absolute difference between the experimental precursor ion mass and the nearest theoretical isotope peak. The search results were grouped by charge state (+1, +2, +3, +4), tryptic status, and modification status (modified and unmodified peptides), resulting in 24 distinct subgroups. In each of these subgroups, the distribution of Xcorr, DeltaCN and DeltaMass values for the direct and decoy database hits was obtained, then the direct and decoy subsets were separated by discriminant analysis. Outlier points in the two distributions were discarded. Full separation of the direct and decoy subsets is not generally possible so the discriminant score was set such that a false discovery rate of less than 1% was determined based on the number of accepted decoy database peptides (number of decoy database hits/number of filtered peptides identified × 100). This procedure was independently performed on each data subset, resulting in a false discovery rate independent of tryptic status, modification status, or charge state. In addition, a minimum peptide length of seven amino acids residues was imposed and protein identification required the matching of at least two peptides per protein. Such criteria resulted in the elimination of most decoy database hits.

Untargeted LC-MS profiling of tissues from *Abhd3*$^{-/-}$ mice. Metabolomic profiling experiments were performed as previously described[9]. except with slight modifications to the LC gradient. The flow rate was 0.5 ml/min and the gradient consisted of 5 min 0% B, a linear increase to 100% B over 15 min, followed by an isocratic gradient of 100% B for 12 min before equilibrating for 5 min at 0% B (37 min total).

Measurement of tissue fatty acyl-CoA levels. Tissue fatty acyl-CoAs were measured using a previously reported method[10], with slight modifications. Tissues were Dounce homogenized in 0.8 ml 0.1 M KH_2PO_4, 0.8 ml isopropanol, 0.1 ml saturated aqueous ammonium sulfate, and 1.6 ml acetonitrile with 10 nmol C10-CoA internal standard. The sample was vortexed and centrifuged (1,400 x g, 10 min, 4°C). The supernatant was diluted with 8 ml 0.1 M KH_2PO_4. 4 ml of this sample was loaded onto an Oasis HLB 1cc (30 mg) extraction cartridge (Waters) preconditioned with 3 ml acetonitrile and 2 ml 25 mM KH_2PO_4. The cartridge was washed once with water (4 ml) and eluted with 0.5 ml of 40:60 v/v acetonitrile:water containing 15 mM NH_4OH. A portion of the eluant (50 µl) was injected onto an Agilent G6410B QQQ instrument. LC separation was achieved with a Gemini reverse-phase C18 column (5 µm, 4.6 mm x 50 mm, Phenomonex) together with a pre-column (C18, 3.5 µm, 2 mm x 20 mm). Mobile phase A was composed of 95:5 v/v H_2O:MeOH, and mobile phase B was composed of 60:35:5 v/v/v *i*-PrOH:MeOH:H_2O. 0.1% ammonium hydroxide was included in each buffer to assist in ion formation in negative ionization mode. The flow rate for each run started at 0.1 ml/min with 0% B. At 2 min, the flow rate was increased to 0.4 ml/min and increased linearly to 100% B over 6 min. This was followed by an isocratic gradient of 100% B for 9 min at 0.5 ml/min before

equilibrating for 3 min at 0% B at 0.5 ml/min (20 min total per sample). MS analysis was performed with an electrospray ionization (ESI) source. The dwell time for each lipid was set to 200 ms. The capillary was set to 4 kV, the fragmentor was set to 100 V, and the delta EMV was set to –200. The drying gas temperature was 350°C, the drying gas flow rate was 11 l/min, and the nebulizer pressure was 35 psi. Lipids were quantified by measuring the area under the peak in comparison to the unnatural standard. The following MS parameters were used to measure the indicated metabolites (collision energy in V):

Acyl chain	Parent	Daughter	CE
C10	920.2	408	40
C12	948.3	408	40
C14	976.3	408	40
C16	1004.3	408	40
C18	1032.4	408	40
C18:1	1030.4	408	40
C18:2	1028.4	408	40
C20	1060.4	408	40
C20:4	1052.3	408	40
C22:6	1076.3	408	40

Targeted MRM measurements of lysoPL and PL species. Mice were anesthetized with isofluorane, sacrified by decapitation, and tissue portions (~100–200 mg) were harvested and flash frozen in liquid nitrogen. Tissues were Dounce homogenized in 2:1:1 v/v/v $CHCl_3$:MeOH:Tris pH 8.0 (8 ml) containing the appropriate unnatural acyl chain standards. The mixture was vortexed and then centrifuged (1,400 x *g*, 10 min). The organic layer was removed, dried under a stream of N_2, resolubilized in 2:1 v/v $CHCl_3$:MeOH (150 µl). For cell lines, C8161 cells stably expressing epitope-tagged ABHD3, catalytically dead ABHD3-S220A mutant, or GFP were plated at 2 million cells/well in 6-well dishes. After 24 h, the media was aspirated, the

cells were washed once with PBS, and incubated with 1 ml serum free media (DMEM with L-glutamine). After 1 h serum starvation, the media was aspirated and the cells were collected in 1 ml 50 mM Tris pH 8. Lipids from this cell suspension were directly extracted in an additional 3 ml of 2:1 v/v chloroform/methanol. The mixture was vortexed and then centrifuged (1,400 x *g*, 10 min). The organic layer was removed, dried under a stream of N_2, resolubilized in 2:1 v/v $CHCl_3$:MeOH (150 µl). 10 or 30 µl of the resolubilized lipid from mouse tissues or cells, respectively, was injected onto an Agilent G6410B QQQ instrument. For targeted MRM measurements in cells, C8161 cells overexpressing ABHD3 or ABHD3-S220A mutant were plated and harvested in exactly the same way as described in the initial screen. LC separation was achieved with a Gemini reverse-phase C18 column (5 µm, 4.6 mm x 50 mm, Phenomonex) together with a pre-column (C18, 3.5 µm, 2 mm x 20 mm). Mobile phase A was composed of 95:5 v/v H_2O:MeOH, and mobile phase B was composed of 60:35:5 v/v/v *i*-PrOH:MeOH:H_2O. 0.1% ammonium hydroxide and 0.1% formic acid were both included in each buffer to assist in acyl chain fragmentation of either formate-adducted parent masses or $[M–H]^-$ in negative ionization mode for PC, LPC, PE, and LPE.[11] Only 0.1% ammonium hydroxide was included for PA and PG measurements. The flow rate started at 0.1 ml/min. After 3 min, the buffers were immediately changed to 60% B at a flow rate of 0.4 ml/min. The gradient consisted a linear increase to 100% B over 5 min, followed by an isocratic gradient of 100% B for 9 min before equilibrating for 3 min at 0% B (20 min total). MS analysis was performed with an electrospray ionization (ESI) source. The dwell time for each lipid was set to 200 ms. The capillary was set to 4 kV, the fragmentor was set to 100 V, and the delta EMV was set to –200. The drying gas temperature was 350°C, the drying gas flow rate was 11 l min^{-1}, and the nebulizer pressure was 35 psi. Lipids were quantified by measuring the area under the peak in comparison to the

unnatural standard. The following MS parameters were used to measure the indicated metabolites (collision energy in V):

Lipid	Acyl chains	Parent	Daughter	CE
PE	C14/16	662.5	227	30
PE	C14/18:2	686.5	227	30
PE	C14/18:1	688.5	227	30
PE	C14/18	690.5	227	30
PE	C14/20:4	710.5	227	30
PE	C14/22:6	734.5	227	30
PE	C16/16	690.5	255	30
PE	C16/18:2	714.5	255	30
PE	C16/18:1	716.5	255	30
PE	C16/18	718.5	255	30
PE	C16/20:4	738.5	255	30
PE	C16/22:6	762.5	255	30
LPE	C14	424	227	30
LPE	C16	452	255	30
LPE	C18:2	476	279.3	30
LPE	C18:1	478	281.3	30
LPE	C18	480	283.3	30
LPE	C20	508	311.3	30
LPE	C20:4	500	303	30
LPE	C22:6	524	327	30
PC	C14/16	750.5	227	30
PC	C14/18:2	774.5	227	30
PC	C14/18:1	776.5	227	30
PC	C14/18	778.5	227	30
PC	C14/20:4	798.5	227	30
PC	C14/22:6	822.5	227	30
PC	C16/16	778.5	255	30
PC	C16/18:2	802.5	255	30
PC	C16/18:1	804.5	255	30
PC	C16/18	806.5	255	30
PC	C16/20:4	826.5	255	30
PC	C16/22:6	850.5	255	30
PC	C18/18:2	830.5	283	30
PC	C16/18:1	832.5	283	30
PC	C18/18	834.5	283	30
PC	C18/20:4	854.5	283	30
PC	C18/22:6	878.5	283	30
LPC	C14	512	227	30
LPC	C16	538	255	30
LPC	C18:2	564	279	30
LPC	C18:1	566	281	30
LPC	C18	568	283	30

LPC	C20:4	624	303	30
LPC	C22:6	612	327	30
PA	C14/16	619.4	255	30
PA	C14/18:2	643.5	279.3	30
PA	C14/18:1	645.5	281.3	30
PA	C14/18	647.5	283.3	30
PA	C14/20:4	667.5	303	30
PA	C14/22:6	691.4	327	30
PA	C16/16	647.4	255	30
PA	C16/18:2	671.5	279.3	30
PA	C16/18:1	673.5	281.3	30
PA	C16/18	675.5	283.3	30
PA	C16/20:4	695.5	303	30
PA	C16/22:6	719.4	327	30
PA	C18/18:1	701.5	281.3	30
PA	C18/18	703.5	283.3	30
PA	C18/20:4	723.5	303	30
LPA	C14	381	153	30
LPA	C16	409	153	30
LPA	C18:2	433	153	30
LPA	C18:1	435	153	30
LPA	C18	437	153	30
LPA	C20	465	153	30
LPA	C20:4	457	153	30
LPA	C22:6	481	153	30
PG	C14/16	693.5	255	40
PG	C14/18:2	717.5	279.3	40
PG	C14/18:1	719.5	281.3	40
PG	C14/18	721.5	283.3	40
PG	C14/20:4	741.5	303	40
PG	C14/22:6	765.5	327	40
PG	C16/16	721.5	255	40
PG	C16/18:2	745.5	279.3	40
PG	C16/18:1	747.5	281.3	40
PG	C16/18	749.5	283.3	40
PG	C16/20:4	769.5	303	40
PG	C16/22:6	793.5	327	40
PG	C18/18:1	775.6	281.3	40
PG	C18/18	777.6	283.3	40
Fatty acid	C14	227	227	0
Fatty acid	C18:1	281	281	0
Fatty acid	C20:4	303	303	0

Partial purification of ABHD3. Total cell lysates from HEK293T cells transfected with epitope-tagged ABHD3 or ABHD3-S220A, as described above, was directly incubated with TALON metal affinity resin (1 mg/ml protein in PBS, 1.5 mg total protein with 150 µl slurry) for 1 h at room temperature. The resin was washed four times with PBS (1 ml each), and resuspended to a final volume of 1.5 ml of PBS. 100 µg of this suspension was used directly for substrate hydrolysis assays or labeled with FP-Rh (1 µM) on bead, as described above.

Incubation and measurement of azelaoyl-PAF in cells. C8161 cells overexpressing ABHD3 or catalytically dead ABHD3-S220A mutant were plated at 2 million cells/6-well dish. After 24 h, the media was aspirated, the cells were washed once with PBS, and incubated with 1 ml serum free media (DMEM with L-glutamine) containing 10 µM azelaoyl-PAF. After 4 h incubation, the media was aspirated, the cells were washed twice with PBS and then collected in 1 ml 50 mM Tris pH 8. Lipids from this cell suspension were directly extracted in an additional 3 ml of 2:1 v/v chloroform/methanol, and the MRM detection of azelaoyl-PAF was performed exactly as described for lysoPL and PL species, except the additive in both buffers was 0.1% formic acid only and the transition and collision energy were 652.5 > 184 and 30 V, respectively.

Oxidation of lipids with $CuSO_4$. Using previously reported protocols with slight modificiations[12], 1-palmitoyl-2-linoleoyl-glycerol-3-phosphocholine (600 nmol) was incubated in aqueous $CuSO_4$ (2.5 mM in 1.2 ml final volume) or water without $CuSO_4$ at 37°C. After 18 h, the oxidized lipids were extracted in 2:1 v/v chloroform/methanol (3 ml total). The mixture was vortexed and then centrifuged (1,400 x *g*, 10 min). The organic layer was removed, dried under a

stream of N_2, resolubilized in 2:1 v/v $CHCl_3$:MeOH (120 µl) to create a stock of effective concentration 5 mM. 2 µl of this resultant substrate was used as a substrate in the phospholipase assays exactly as described above.

Supplemental References

1. Patricelli, M.P., Giang, D.K., Stamp, L.M. & Burbaum, J.J. Direct visualization of serine hydrolase activities in complex proteomes using fluorescent active site-directed probes. *Proteomics* **1**, 1067-71 (2001).
2. Liu, Y., Patricelli, M.P. & Cravatt, B.F. Activity-based protein profiling: the serine hydrolases. *Proceedings of the National Academy of Sciences of the United States of America* **96**, 14694-9 (1999).
3. Heo, H.J. et al. Synthesis of Lysophosphatidylcholine Analogues Using D-Mannitol as a Chiral Template and Their Biological Activity for Sepsis. *Bulletin of the Korean Chemical Society* **27**, 1149-53 (2006).
4. Bachovchin, D.A. et al. Superfamily-wide portrait of serine hydrolase inhibition achieved by library-versus-library screening. *Proceedings of the National Academy of Sciences of the United States of America* **107**, 20941-6 (2010).
5. Smith, C.A., Want, E.J., O'Maille, G., Abagyan, R. & Siuzdak, G. XCMS: processing mass spectrometry data for metabolite profiling using nonlinear peak alignment, matching, and identification. *Analytical Chemistry* **78**, 779-87 (2006).
6. Martin, B.R. & Cravatt, B.F. Large-scale profiling of protein palmitoylation in mammalian cells. *Nat Methods* **6**, 135-8 (2009).
7. Washburn, M.P., Wolters, D. & Yates, J.R., 3rd. Large-scale analysis of the yeast proteome by multidimensional protein identification technology. *Nature Biotechnology* **19**, 242-7 (2001).

8. Yates, J.R., 3rd, Eng, J.K., McCormack, A.L. & Schieltz, D. Method to correlate tandem mass spectra of modified peptides to amino acid sequences in the protein database. *Analytical Chemistry* **67**, 1426-36 (1995).

9. Saghatelian, A. et al. Assignment of endogenous substrates to enzymes by global metabolite profiling. *Biochemistry* **43**, 14332-9 (2004).

10. Magnes, C., Sinner, F.M., Regittnig, W. & Pieber, T.R. LC/MS/MS method for quantitative determination of long-chain fatty acyl-CoAs. *Analytical Chemistry* **77**, 2889-94 (2005).

11. Nakanishi, H., Iida, Y., Shimizu, T. & Taguchi, R. Analysis of oxidized phosphatidylcholines as markers for oxidative stress, using multiple reaction monitoring with theoretically expanded data sets with reversed-phase liquid chromatography/tandem mass spectrometry. *J Chromatogr B Analyt Technol Biomed Life Sci* **877**, 1366-74 (2009).

12. Davies, S.S. et al. Oxidized alkyl phospholipids are specific, high affinity peroxisome proliferator-activated receptor gamma ligands and agonists. *Journal of Biological Chemistry* **276**, 16015-23 (2001).

13. Su, A.I. et al. Large-scale analysis of the human and mouse transcriptomes. *Proceedings of the National Academy of Sciences of the United States of America* **99**, 4465-70 (2002).

SUPPLEMENTARY RESULTS

Supplementary Figure Legends

Supplementary Fig. 1. Schematic depiction of a metabolomics-coupled enzyme library screen for substrate discovery. HEK293T cells are transfected with enzymes and then metabolomes are harvested by chloroform/methanol extraction. Comparison of all metabolomes at a given *m/z* reveals metabolites whose levels are selectively elevated (candidate products, shown in green for enzyme 2) or selectively depleted (candidate substrates, shown in blue for enzyme 1) in a specific enzyme-transfected cell preparation.

Supplementary Fig. 2. CES2 overexpression depletes a metabolite with *m/z* = 391 and retention time ~23 min. (**a**) FP-Rh labeling profiles of mock- versus CES2-transfected HEK293T cells. Arrowhead designates FP-Rh-labeled CES2 protein. (**b**) Overlaid extracted ion chromatograms at *m/z* = 390.5–391.5 of HEK293T cells transfected with CES2 (red trace) versus other enzymes (blue traces).

Supplementary Fig. 3. FP-Rh labeling profiles of mock- versus ABHD3-transfected HEK293T cells. Arrowhead designates FP-Rh-labeled ABHD3 protein. A cropped portion of this gel is shown in **Fig. 1a**.

Supplementary Fig. 4. Elevation of metabolite with *m/z* = 524 is dependent on ABHD3 catalytic activity. (**a, b**) FP-Rh labeling profiles (*top panels*) of C8161 (**a**) or MUM2C (**b**) cells

stably overexpressing epitope-tagged ABHD3, a catalytically dead ABHD3-S220A mutant, or GFP. *Bottom panels*: Immunoblotting using an antibody against 6xHIS epitope tag appended to the C-terminus of ABHD3 protein. Arrowhead designates FP-Rh-labeled ABHD3 (note that no FP-Rh labeling is observed for the catalytically dead ABHD3-S220A mutant, even though this protein is expressed at equivalent or greater levels than wild type ABHD3 as judged by 6xHIS immunoblotting). For the FP-Rh gel in (**a**), cell lysates were also treated with PNGaseF to deglycosylate co-migrating serine hydrolases. (**c**) Relative peak area of *m/z* = 524 in C8161 cells stably overexpressing ABHD3 (blue), ABHD3-S220A (red), or GFP (green). Data are presented as mean ± standard error; n = 3/group; ** $P < 0.01$, *** $P < 0.001$.

Supplementary Fig. 5. Endogenous *m/z* = 524 from C8161 cells overexpressing ABHD3 (blue trace) co-elutes with a synthetic C18-LPC standard (red trace).

Supplementary Fig. 6. Targeted MRM measurements of lysophosphatidylcholines (LPCs) from C8161 cells overexpressing ABHD3 (dark grey), ABHD3-S220A (black), or GFP (light grey). LPC species are indicated by C#, where # is the acyl chain length. Data are presented as mean ± standard error; n = 3/group; * $P < 0.05$, ** $P < 0.01$, *** $P < 0.001$.

Supplementary Fig. 7. Myristic acid levels in C8161 cells stably overexpressing ABHD3, ABHD3-S220A, or GFP. Data are presented as mean ± standard error; n = 3/group.

Supplementary Fig. 8. FP-Rh labeling profiles of brain membranes from *Abhd3*$^{+/+}$ or *Abhd3*$^{-/-}$ mice. ABHD3 is indicated by the arrowhead. Two separate mice are shown for each genotype.

Supplementary Fig. 9. Tissue distribution of ABHD3 in mice. (**a**) ABHD3 activity in different tissues as determined by ABPP-MudPIT and reported previously[4]. (**b**) ABHD3 mRNA expression in different tissues, as determined by Affymetrix DNA microarrays and reported previously[13].

Supplementary Fig. 10. MS/MS fragmentation (collision energy 30 V) of *m/z* = 468 (**a**), 730.5 (**b**), 754.5 (**c**), and 778.5 (**d**), four metabolites that were elevated in kidney tissue from *Abhd3*$^{-/-}$ mice. All four metabolites all generated a daughter fragment of *m/z* = 184.1 characteristic of phosphocholine, and *m/z* = 468 also generated a daughter ion with *m/z* = 104.1 indicative of choline.

Supplementary Fig. 11. Substrate profile of partially purified ABHD3. (**a**) Kyte-Doolittle hydropathy plot for mouse ABHD3, using a window size of 11 amino acids. The N-terminal transmembrane (TM) domain is indicated. (**b**) FP-Rh labeling (*top left*), 6xHIS Western blot (*bottom left*), or azPAF hydrolysis activity (*right*) of C8161 membrane or soluble fractions overexpressing epitope-tagged ABHD3 or catalytically inactive ABHD3-S220A mutant. The membrane and soluble fractions were separated by centrifugation at 100,000 x g. For the FP-Rh gel, samples were treated with PNGaseF to remove a co-migrating band. For azPAF hydrolysis activity, rates were normalized to that present in the membrane fraction of ABHD3-overexpressing cells (lane 2). (**c**) FP-Rh labeling (*top left*) or 6xHIS Western blot (*bottom left*) of total cell lysates from HEK293T cells transiently transfected with epitope-tagged ABHD3 or catalytically inactive ABHD3-S220A mutant. For lanes 3 and 4, ABHD3 was partially purified

on metal-affinity resin as described in the **Supplementary Methods**. *Right*: Hydrolysis activities for various PC species using partially purified ABHD3 or ABHD3-S220A. Activities are normalized relative to azPAF which is set to 100%. (**d**) Hydrolysis activities for various PC species in C8161 cell lines stably overexpressing ABHD3 or the catalytically inactive ABHD3-S220A mutant, or HEK293T cell lines transiently transfected with ABHD3 or empty vector (mock). Activities are normalized relative to azPAF which is set to 100%. The graph for C8161 cell lines is derived from **Supplemental Table 3**. Data are presented as mean ± standard error; n = 3/group; * $P < 0.05$, ** $P < 0.01$, *** $P < 0.001$ for ABHD3 versus ABHD3-S220A, or ABHD3 versus mock.

Supplementary Fig. 12. Formation of C16-LPC using lysates from stably transfected C8161 cells as the protein source. The substrate was oxidized C16/18:2-PC (2.5 mM $CuSO_4$, 18 h, 37°C) or unoxidized C16/18:2-PC (water, 18 h, 37°C). N.S., not significant. Lysates from cells overexpressing ABHD3 are shown in black, and those overexpressing catalytically dead ABHD3-S220A mutant are shown in grey. Data are presented as mean ± standard error; n = 3–4/group; * $P < 0.05$, ** $P < 0.01$, *** $P < 0.001$ for ABHD3 versus ABHD3-S220A.

Supplementary Fig. 13. Dendrogram showing the primary sequence alignment of the human mammalian metabolic SHs, where alignment was generated by anchoring sequences at the site of their catalytic Ser residues. ABHD1–3 are highlighted in red.

Supplementary Table 1. Spectral counts using untargeted MS-based proteomics, as described in the supplementary methods, of all proteins detected in brain membranes of *Abhd3*$^{+/+}$ or *Abhd3*$^{-/-}$

mice. Only those proteins with average 10 spectral counts in brains from *Abhd3*$^{+/+}$ mice, and detected in all three *Abhd3*$^{+/+}$ replicates, are shown. n = 3/group. A selected subset of this table is show in **Fig. 2a**.

Supplementary Table 2. Targeted MRM measurements of lipids from various tissues of *Abhd3*$^{+/+}$ (WT) or *Abhd3*$^{-/-}$ (KO) mice. Data are presented as means and SEM in units of nmol/g except for plasma, where units are in nmol/ml; n = 3–4/group. Fold indicates fold-change in *Abhd3*$^{-/-}$ versus *Abhd3*$^{+/+}$ tissues. Shown in red are metabolites with fold-change > 2 and $P < 0.05$.

Supplementary Table 3. Hydrolysis activity of C8161 cell lysates overexpressing ABHD3 or the catalytically dead ABHD3-S220A mutant. Total cell lysate (30 μg) was incubated with the indicated substrate (100 μM) in PBS for 1 h, and products were extracted using chloroform/methanol and analyzed by LC-MS. Hydrolysis rates were quantified by comparison to unnatural lysophospholipid or fatty acid standards. Substrates are indicated by C#/##, where the # indicates the sn-1 acyl chain and ## indicates the sn-2 acyl chain. ND, not detected. Data are presented as mean ± standard error in units of pmol/min/mg; n = 3/group. For entries 15–30, PLA1 activity was not detected.

Supplementary Table 1.

Please see accompanying Excel spreadsheet.

Supplementary Table 2.

Tissue	Lipid	Acyl chain(s)	Fold	T-test	WT Avg.	KO Avg.	WT SEM	KO SEM
Kidney	PC	C14/16	2.3	0.0002	4.1	9.6	0.3	0.2
Kidney	PC	C14/18:2	2.2	0.0043	0.8	1.7	0.1	0.0
Kidney	PC	C14/18:1	2.4	0.0043	0.4	0.9	0.1	0.0
Kidney	PC	C14/20:4	8.4	0.0000	0.1	1.1	0.0	0.0
Kidney	PC	C14/22:6	6.0	0.0006	0.4	2.4	0.0	0.1
Kidney	PC	C16/16	0.9	0.1417	110.0	98.0	4.2	4.7
Kidney	PC	C16/18:2	0.8	0.0970	32.0	26.0	1.8	2.0
Kidney	PC	C16/18:1	1.0	1.0000	13.0	13.0	1.2	1.3
Kidney	PC	C16/18	0.8	0.2881	5.6	4.6	0.7	0.3
Kidney	PC	C16/20:4	0.8	0.3898	21.0	18.0	3.2	1.3
Kidney	PC	C16/22:6	1.0	0.6393	30.0	32.0	2.1	0.9
Kidney	PC	C18/18:2	1.1	0.2567	18.0	20.0	0.8	1.1
Kidney	PC	C18/18:1	1.1	0.4070	8.2	9.1	0.6	0.8
Kidney	PC	C18/20:4	1.2	0.2879	5.3	6.2	0.5	0.5
Kidney	PC	C18/22:6	1.1	0.2715	3.0	3.4	0.2	0.1
Kidney	PC	C18:1/18:2	0.6	0.5536	4.8	2.9	2.0	2.1
Kidney	PC	C18:1/18:1	1.1	0.5040	4.3	4.7	0.3	0.5
Kidney	PC	C18:1/20:4	1.0	0.8782	3.7	3.8	0.2	0.5
Kidney	PC	C18:1/22:6	1.0	0.8767	1.2	1.2	0.1	0.0
Kidney	PC	C18:1/18:2	1.0	0.6856	9.1	9.4	0.3	0.6
Kidney	LPC	C14	3.0	0.0034	0.94	2.8	0.067	0.17
Kidney	LPC	C16	1.0	0.9620	340	340	24	22
Kidney	LPC	C18	1.0	0.8228	140	140	15	12
Kidney	LPC	C20	1.1	0.4303	1.4	1.6	0.18	0.072
Kidney	LPC	C22	1.0	0.6850	0.43	0.45	0.025	0.033
Kidney	LPC	C24	1.1	0.8014	0.32	0.34	0.067	0.01
Kidney	LPC	C18:2	0.7	0.0640	110	77	7.3	8.4
Kidney	LPC	C18:1	0.8	0.2488	45	37	4.7	4
Kidney	LPC	C20:4	1.0	0.7583	14	14	1.7	1.3
Kidney	LPC	C22:6	0.9	0.7598	3.4	3.2	0.3	0.5
Kidney	Acyl-CoA	C14	0.8	0.5700	1.9	1.5	0.5	0.2
Kidney	Acyl-CoA	C16	0.8	0.3261	2.7	2.0	0.5	0.1
Kidney	Acyl-CoA	C18:2	0.8	0.2663	5.0	4.2	0.5	0.2
Kidney	Acyl-CoA	C18:1	0.8	0.3727	2.9	2.3	0.5	0.3
Kidney	Acyl-CoA	C18	0.8	0.1167	1.0	0.8	0.1	0.1
Kidney	Acyl-CoA	C20:4	0.8	0.0248	5.0	4.2	0.1	0.2
Kidney	Fatty acid	C14	1.3	0.2675	4.1	5.2	0.71	0.26
Kidney	Fatty acid	C18:1	1.1	0.7347	37	41	9.3	5.7
Kidney	Fatty acid	C20:4	0.8	0.2875	17	14	1.8	1.1
Brain	PC	C14/16	2.0	0.0031	7.8	16.0	0.9	0.8
Brain	PC	C14/18:2	2.3	0.0156	0.1	0.2	0.0	0.0
Brain	PC	C14/18:1	2.0	0.0002	1.4	2.8	0.1	0.2
Brain	PC	C14/20:4	2.8	0.0013	0.1	0.3	0.0	0.0
Brain	PC	C14/22:6	3.4	0.0051	0.1	0.4	0.0	0.1
Brain	PC	C16/16	1.0	0.9024	47.0	46.0	2.6	1.2

Brain	PC	C16/18:2	1.1	0.4282	2.9	3.1	0.2	0.2
Brain	PC	C16/18:1	1.0	1.0000	29.0	29.0	0.6	0.1
Brain	PC	C16/18	1.0	0.8076	8.4	8.3	0.5	0.2
Brain	PC	C16/20:4	1.0	0.7945	7.2	7.4	0.8	0.2
Brain	PC	C16/22:6	1.1	0.1468	9.1	10.0	0.5	0.5
Brain	PC	C18/18:2	1.0	0.6083	0.7	0.6	0.0	0.0
Brain	PC	C18/18:1	1.0	0.2886	14.0	14.0	0.3	0.2
Brain	PC	C18/20:4	1.0	0.7507	1.7	1.7	0.1	0.0
Brain	PC	C18/22:6	1.0	0.7767	1.5	1.5	0.1	0.0
Brain	LPC	C14	3.2	0.0050	0.2	0.7	0.1	0.0
Brain	LPC	C16	1.3	0.1999	46.0	59.0	7.3	3.2
Brain	LPC	C18	1.3	0.2524	18.0	23.0	3.1	1.6
Brain	LPC	C20	1.5	0.0386	0.4	0.6	0.0	0.1
Brain	LPC	C22	1.2	0.2384	0.2	0.3	0.0	0.0
Brain	LPC	C24	1.1	0.4472	0.3	0.3	0.0	0.0
Brain	LPC	C18:2	1.2	0.2619	1.8	2.2	0.1	0.3
Brain	LPC	C18:1	1.2	0.2991	19.0	23.0	2.6	0.8
Brain	LPC	C20:4	1.1	0.5157	1.7	1.9	0.2	0.1
Brain	LPC	C22:6	1.0	0.9341	0.5	0.5	0.0	0.0
Brain	PE	C14/16	1.4	0.1327	0.67	0.91	0.1	0.068
Brain	PE	C14/18:2	2.6	0.0181	0.23	0.59	0.058	0.017
Brain	PE	C14/18:1	3.6	0.0008	2	7.2	0.23	0.38
Brain	PE	C14/20:4	1.6	0.0161	0.7	1.2	0.067	0.018
Brain	PE	C14/22:6	5.7	0.0106	0.55	3.1	0.066	0.3
Brain	PE	C16/16	0.9	0.2739	27	24	0.87	1.7
Brain	PE	C16/18:2	1.0	0.9598	11	10	0.35	1.5
Brain	PE	C16/18:1	0.9	0.4434	110	100	6.3	2.6
Brain	PE	C16/18	1.1	0.6659	16	17	0.84	2
Brain	PE	C16/20:4	1.1	0.4673	99	110	8.4	6.8
Brain	PE	C16/22:6	1.0	0.9400	340	340	15	39
Brain	LPE	C14	2.6	0.0000	0.69	1.8	0.028	0.02
Brain	LPE	C16	1.0	0.8023	290	280	26	33
Brain	LPE	C18:2	0.9	0.3194	14	12	1.3	0.99
Brain	LPE	C18:1	0.8	0.3949	440	370	66	20
Brain	LPE	C18	0.8	0.2388	700	530	100	59
Brain	LPE	C20	0.9	0.8214	17	16	5.3	1.4
Brain	LPE	C20:4	0.9	0.8161	45	42	6.8	7.7
Brain	LPE	C22:6	1.0	1.0000	17	17	1.5	2.7
Brain	PA	C14/16	1.5	0.0464	4	6.1	0.43	0.55
Brain	PA	C14/18:2	3.3	0.0049	0.15	0.48	0.033	0.044
Brain	PA	C14/18:1	5.3	0.0000	3.9	21	0.55	0.43
Brain	PA	C14/18	2.8	0.0010	0.61	1.7	0.039	0.075
Brain	PA	C14/20:4	4.0	0.0091	0.75	3	0.14	0.31
Brain	PA	C14/22:6	1.8	0.0090	0.38	0.7	0.032	0.05
Brain	PA	C16/16	0.9	0.4069	50	43	5.5	5.5
Brain	PA	C16/18:2	0.9	0.5903	25	21	5.5	2.1
Brain	PA	C16/18:1	0.9	0.5682	340	310	40	12
Brain	PA	C16/18	1.0	0.7958	19	19	2.3	0.9
Brain	PA	C16/20	1.2	0.3033	37	43	4.3	2.1
Brain	PA	C16/20:4	0.9	0.4366	140	130	14	6
Brain	PA	C16/22:6	0.9	0.3227	21	18	1.5	2
Brain	PA	C18/18:1	0.8	0.2434	260	210	32	15
Brain	PA	C18/18	0.6	0.4340	19	11	8.3	0.83

Brain	PA	C18/20:4	0.8	0.1793	99	79	10	6.2
Brain	LPA	C14	1.3	0.3974	0.005	0.006	0.001	0.001
Brain	LPA	C16	1.1	0.7848	0.129	0.137	0.024	0.008
Brain	LPA	C18:2	1.2	0.5699	0.013	0.014	0.002	0.002
Brain	LPA	C18:1	0.9	0.3885	0.262	0.234	0.022	0.018
Brain	LPA	C18	1.0	1.0000	0.199	0.199	0.012	0.007
Brain	LPA	C20	0.8	0.2970	0.028	0.023	0.004	0.002
Brain	LPA	C20:4	0.9	0.3747	0.152	0.137	0.012	0.010
Brain	LPA	C22:6	0.9	0.3642	0.038	0.036	0.001	0.002
Brain	Acyl-CoA	C14	1.1	0.6667	0.6	0.7	0.0	0.1
Brain	Acyl-CoA	C16	0.8	0.3492	5.9	4.5	0.4	1.1
Brain	Acyl-CoA	C18:2	0.7	0.4208	1.2	0.8	0.3	0.1
Brain	Acyl-CoA	C18:1	0.8	0.5998	7.0	5.7	1.3	1.3
Brain	Acyl-CoA	C18	0.9	0.7592	2.1	1.9	0.4	0.5
Brain	Acyl-CoA	C20:4	0.9	0.4685	6.4	5.9	0.4	0.3
Brain	Fatty acid	C14	1.3	0.1952	3.5	4.5	0.29	0.15
Brain	Fatty acid	C18:1	1.0	0.8999	36	35	2.4	5.4
Brain	Fatty acid	C20:4	1.2	0.1331	110	120	3.6	1.7
Liver	PC	C14/16	0.9	0.7496	0.47	0.41	0.023	0.16
Liver	PC	C14/18:2	3.0	0.0002	0.55	1.7	0.099	0.07
Liver	PC	C14/18:1	1.9	0.0164	0.23	0.44	0.016	0.046
Liver	PC	C14/20:4	6.0	0.0025	0.15	0.9	0.092	0.026
Liver	PC	C14/22:6	5.3	0.0033	0.12	0.61	0.059	0.0082
Liver	PC	C16/16	0.9	0.1778	3.5	3.3	0.13	0.11
Liver	PC	C16/18:2	1.0	0.5041	14	14	0.25	0.25
Liver	PC	C16/18:1	0.9	0.2686	7.6	6.7	0.33	0.56
Liver	PC	C16/20:4	1.1	0.2453	8.1	8.7	0.44	0.16
Liver	PC	C16/22:6	1.0	0.6283	4.6	4.5	0.13	0.11
Liver	PC	C18/18:2	1.1	0.3243	13	13	0.45	0.38
Liver	PC	C18/18:1	0.9	0.2070	2.3	2.1	0.13	0.13
Liver	PC	C18/20:4	1.2	0.0460	2.3	2.8	0.15	0.11
Liver	PC	C18/22:6	1.0	1.0000	1.1	1.1	0.049	0.085
Liver	LPC	C14	4.1	0.0018	2.3	9.3	1.6	0.55
Liver	LPC	C16	1.1	0.4931	910	970	140	78
Liver	LPC	C18	1.1	0.3449	350	390	68	33
Liver	LPC	C20	1.6	0.0273	2.9	4.6	0.94	0.68
Liver	LPC	C22	1.1	0.6805	1.2	1.3	0.38	0.16
Liver	LPC	C24	1.1	0.6950	0.82	0.89	0.19	0.28
Liver	LPC	C18:2	1.0	0.7955	250	260	65	22
Liver	LPC	C18:1	1.0	0.7749	150	140	30	25
Liver	LPC	C20:4	1.2	0.4297	59	69	19	15
Liver	LPC	C22:6	1.6	0.0286	2.9	4.6	0.94	0.68
Liver	PE	C14/16	1.1	0.7391	0.067	0.073	0.014	0.0091
Liver	PE	C14/18:2	2.8	0.0008	0.15	0.43	0.026	0.009
Liver	PE	C14/18:1	1.7	0.0666	0.068	0.11	0.0064	0.017
Liver	PE	C14/20:4	4.3	0.0003	0.11	0.46	0.03	0.015
Liver	PE	C14/22:6	4.3	0.0025	0.3	1.3	0.11	0.024
Liver	PE	C16/16	1.0	0.8829	0.5	0.51	0.053	0.057
Liver	PE	C16/18:2	1.1	0.0792	20	22	1	0.79
Liver	PE	C16/18:1	0.9	0.3815	6.5	5.8	1	0.63
Liver	PE	C16/18	1.0	0.9247	0.75	0.76	0.051	0.11

Liver	PE	C16/20:4	1.0	0.5715	40	42	1.4	2.2
Liver	PE	C16/22:6	1.2	0.0315	83	100	4.6	4.9
Liver	LPE	C14	2.3	0.0019	0.98	2.3	0.082	0.17
Liver	LPE	C16	1.3	0.2660	1000	1300	180	75
Liver	LPE	C18:2	1.4	0.2016	160	240	44	13
Liver	LPE	C18:1	1.2	0.4759	450	520	75	49
Liver	LPE	C18	1.4	0.2227	880	1200	190	100
Liver	LPE	C20:4	1.2	0.5197	130	160	31	33
Liver	LPE	C22:6	1.7	0.0724	13	22	3.4	1.4
Liver	PG	14/16	5.7	0.0106	0.048	0.27	0.036	0.019
Liver	PG	14/18:2	7.5	0.0001	0.019	0.15	0.0028	0.0048
Liver	PG	C16/16	1.1	0.7687	1.5	1.8	0.59	0.39
Liver	PG	C16/18:2	1.3	0.3134	12	16	2.9	1.2
Liver	PG	C16/18:1	1.3	0.4095	32	40	7.3	5.3
Liver	PG	C16/18	1.2	0.4973	1.9	2.3	0.34	0.29
Liver	PG	C16/20:4	1.1	0.6463	1.2	1.3	0.25	0.1
Liver	PG	C16/22:6	1.2	0.5813	0.28	0.34	0.084	0.028
Liver	PG	C18/18:1	0.9	0.7956	2.6	2.4	0.37	0.59
Liver	PG	C18/20:4	1.1	0.5243	1.5	1.7	0.22	0.17
Plasma	PC	C14/16	1.3	0.2030	0.0064	0.0085	0.0015	0.0006
Plasma	PC	C14/18:2	5.5	0.0000	0.015	0.083	0.0031	0.0031
Plasma	PC	C14/18:1	2.5	0.0044	0.0066	0.016	0.0016	0.0019
Plasma	PC	C14/20:4	7.0	0.0002	0.0029	0.02	0.00067	0.0015
Plasma	PC	C14/22:6	7.1	0.0001	0.002	0.015	0.00058	0.00017
Plasma	LPC	C14	4.7	0.0004	2.5	12	0.11	0.64

Supplementary Table 3.

Entry	Substrate	Product	ABHD3	ABHD3-S220A	P-value
1	C14/16-PC	C14-LPC	15 ± 4	7 ± 2	0.0451
	C14/16-PC	C16-LPC	18 ± 2	7 ± 1	0.0081
2	C14/18:2-PC	C14-LPC	17 ± 2	5 ± 1	0.0067
	C14/18:2-PC	C18:2-LPC	69 ± 9	4 ± 1	0.0078
3	C14/20:4-PC	C14-LPC	16 ± 2	12 ± 2	0.0453
	C14/20:4-PC	C20:4-LPC	59 ± 10	1 ± 0.3	0.0098
4	C14/22:6-PC	C14-LPC	20 ± 3	12 ± 3	0.0224
	C14/22:6-PC	C22:6-LPC	182 ± 16	11 ± 1	0.0030
5	C16/18:2-PC	C16-LPC	5 ± 1	4 ± 1	> 0.05
	C16/18:2-PC	C18:2-PC	4 ± 1	4 ± 1	> 0.05
6	C16/20:4-PC	C16-LPC	12 ± 1	12 ± 1	> 0.05
	C16/20:4-PC	C20:4-LPC	6 ± 1	7 ± 1	> 0.05
7	C12/12-PC	C12-LPC	1800 ± 300	60 ± 10	0.0104
8	C14/14-PC	C14-LPC	60 ± 3	24 ± 2	0.0017
9	C15/15-PC	C15-LPC	25 ± 4	18 ± 4	> 0.05
10	C16/16-PC	C16-LPC	30 ± 5	30 ± 9	> 0.05
11	C14/14-PG	C14-LPG	68 ± 17	15 ± 3	0.0299
12	C14/14-PE	C14-LPE	ND	ND	
13	C14/14-PA	C14-LPA	ND	ND	
14	C14/14-PS	C14-LPS	ND	ND	
15	C18/2-PC	C18-LPC	60 ± 3	18 ± 4	0.0021
16	C18/5-PC	C18-LPC	250 ± 20	19 ± 1	0.0030
17	C18/6-PC	C18-LPC	390 ± 30	22 ± 1	0.0019
18	C18/8-PC	C18-LPC	320 ± 30	18 ± 2	0.0043
19	C18/9-PC	C18-LPC	67 ± 9	7 ± 0.4	0.0082
20	C18/10-PC	C18-LPC	29 ± 9	2 ± 0.5	0.0352
21	C18/12-PC	C18-LPC	7 ± 0.4	1 ± 0.3	0.0000
22	C18/14-PC	C18-LPC	5 ± 0.4	2 ± 0.1	0.0049
23	C18/16-PC	C18-LPC	2.4 ± 0.2	2.1 ± 0.2	> 0.05
24	PAF	lysoPAF	210 ± 10	100 ± 8	0.0001
25	C16-alk/4:1-PC	lysoPAF	100 ± 15	10 ± 1	0.0085
26	C16/5-COOH-PC	16-LPC	42 ± 3	27 ± 2	0.0049
27	C16/5-CHO-PC	16-LPC	390 ± 40	190 ± 50	0.0066
28	C16/9-COOH-PC	16-LPC	670 ± 80	50 ± 20	0.0046
29	C16/9-CHO-PC	16-LPC	490 ± 15	30 ± 2	0.0003
30	azPAF	lysoPAF	1560 ± 50	76 ± 7	0.0002

Supplementary Fig. 1

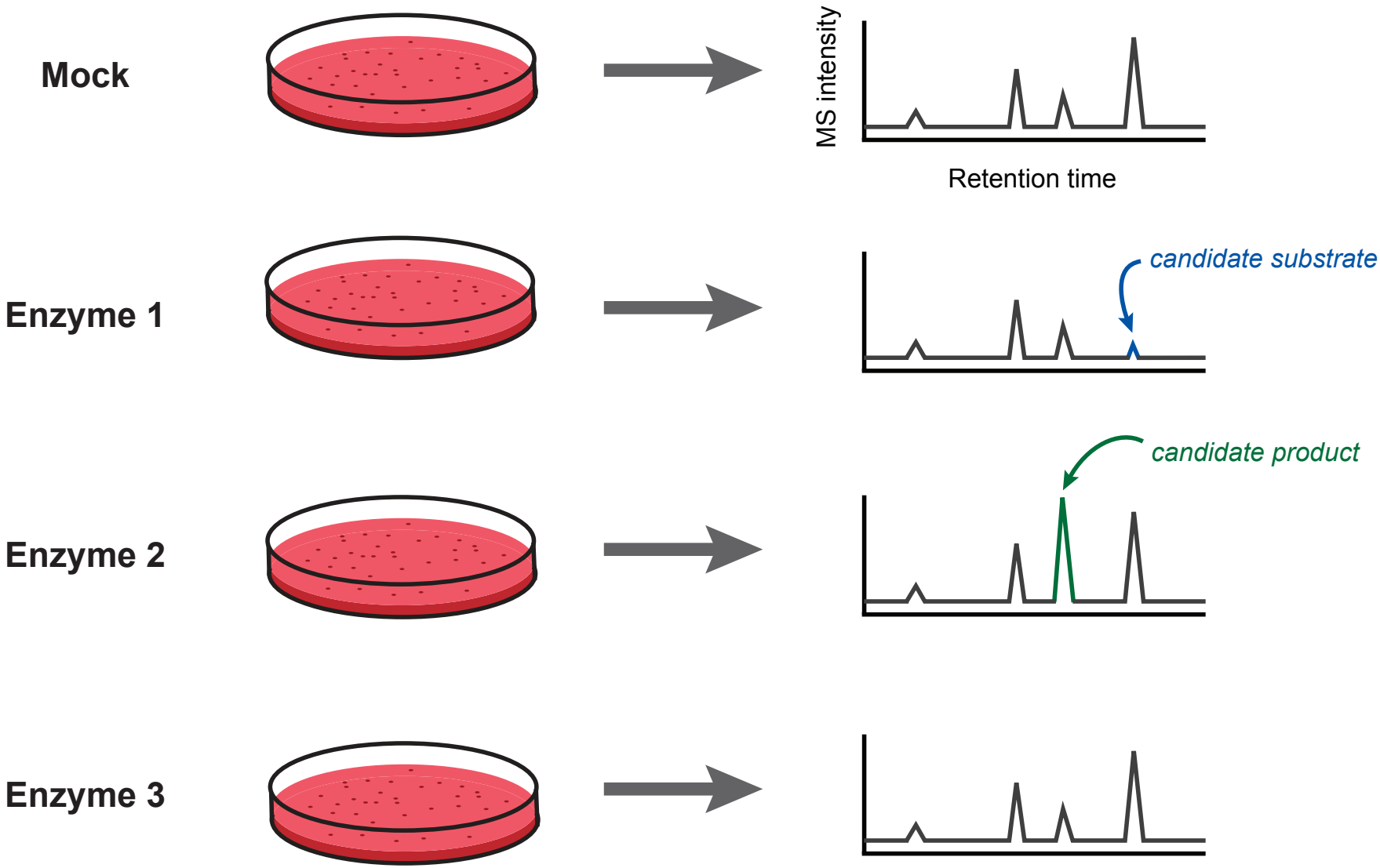

Supplementary Fig. 2

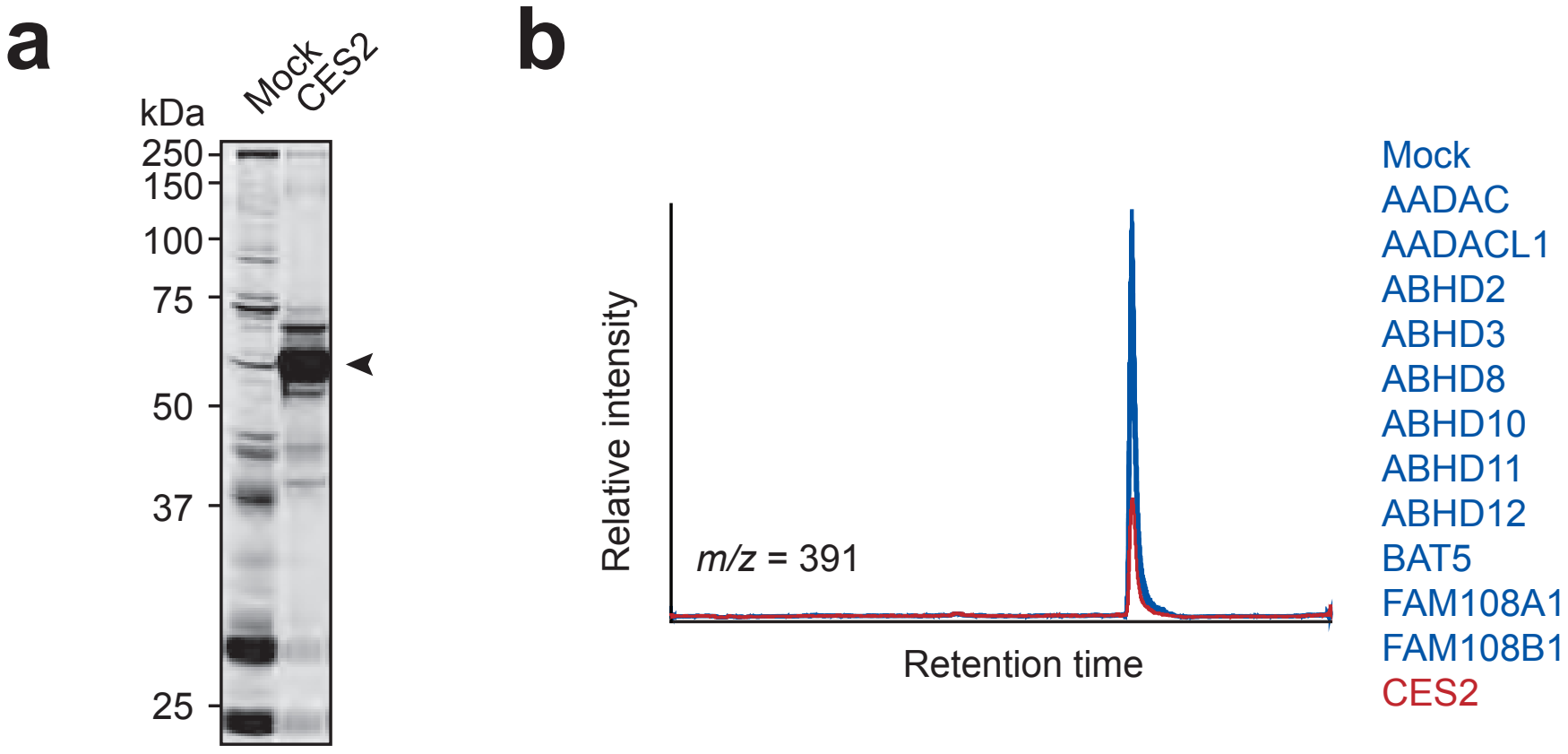

Supplementary Fig. 3

Supplementary Fig. 4

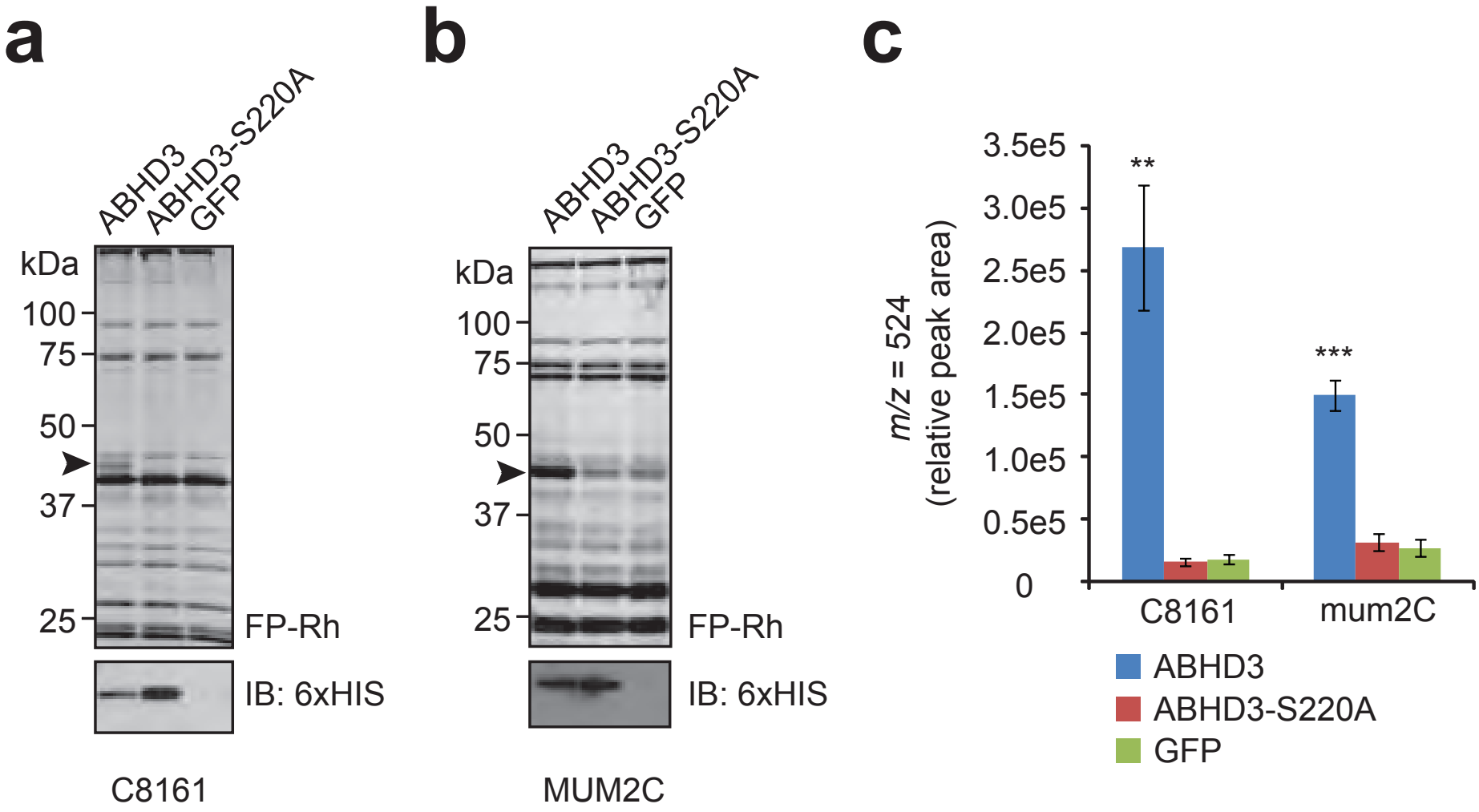

Supplementary Fig. 5

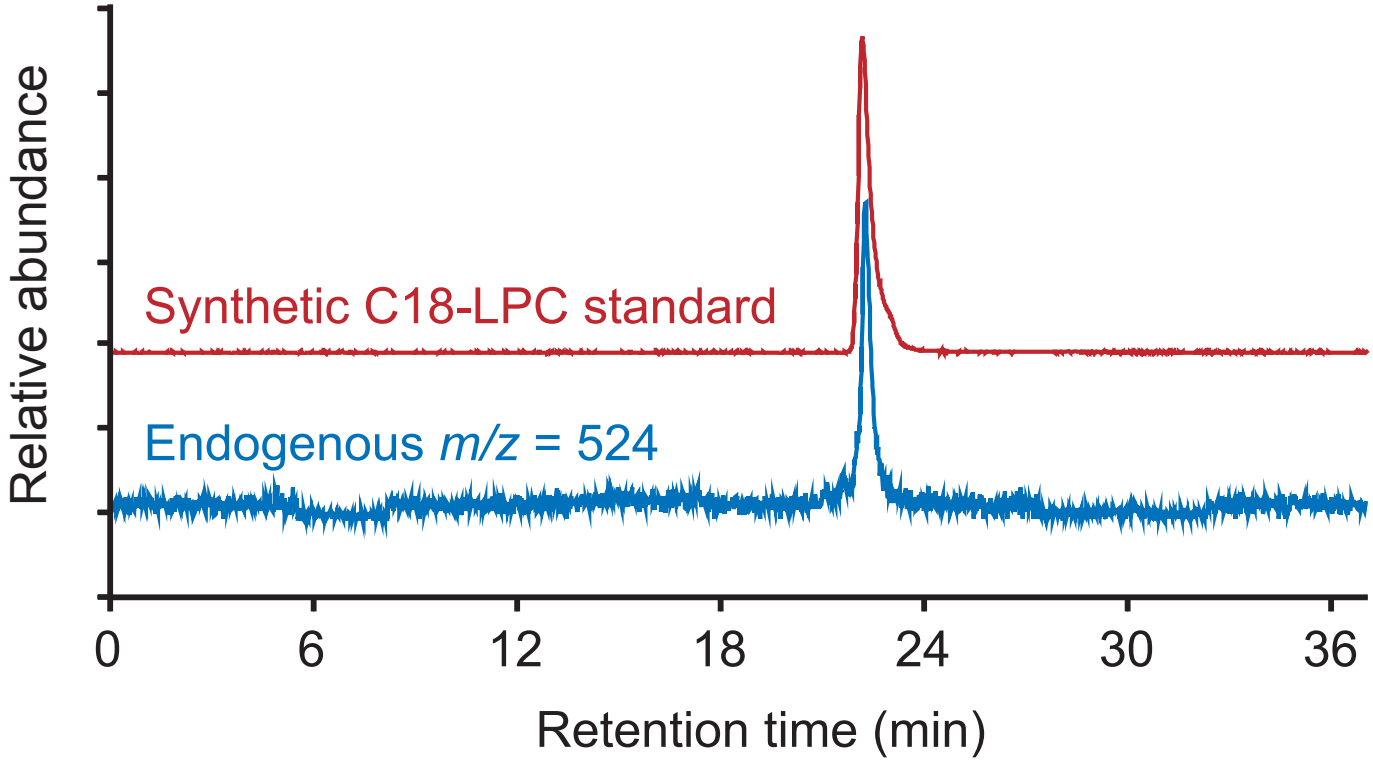

Supplementary Fig. 6

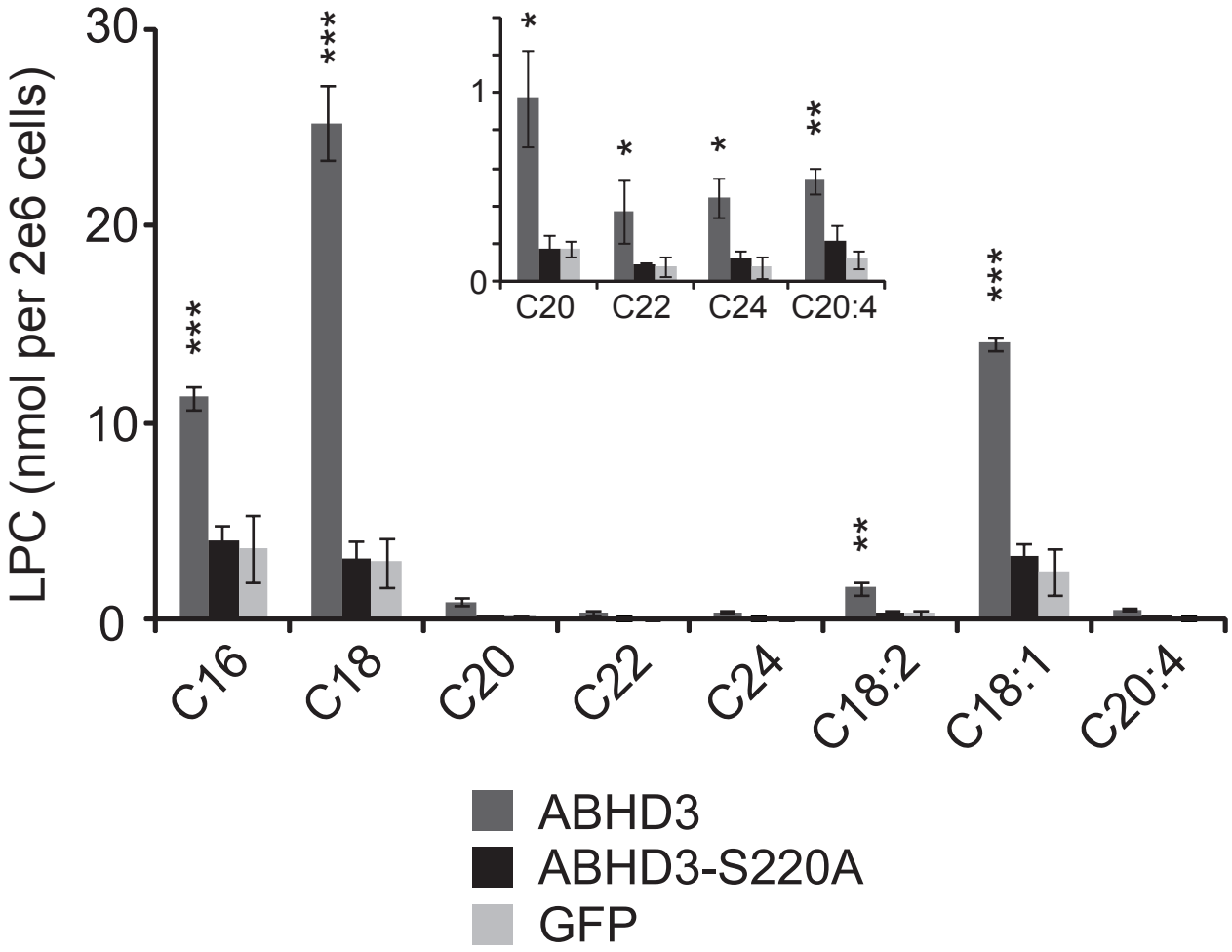

Supplementary Fig. 7

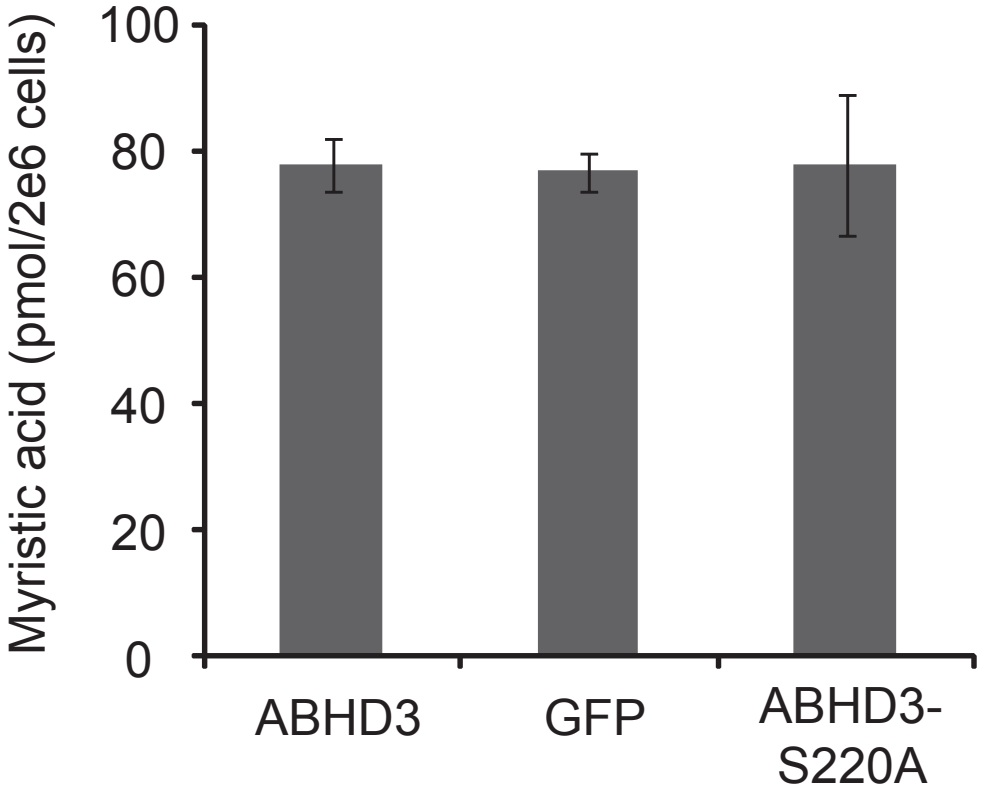

Supplementary Fig. 8

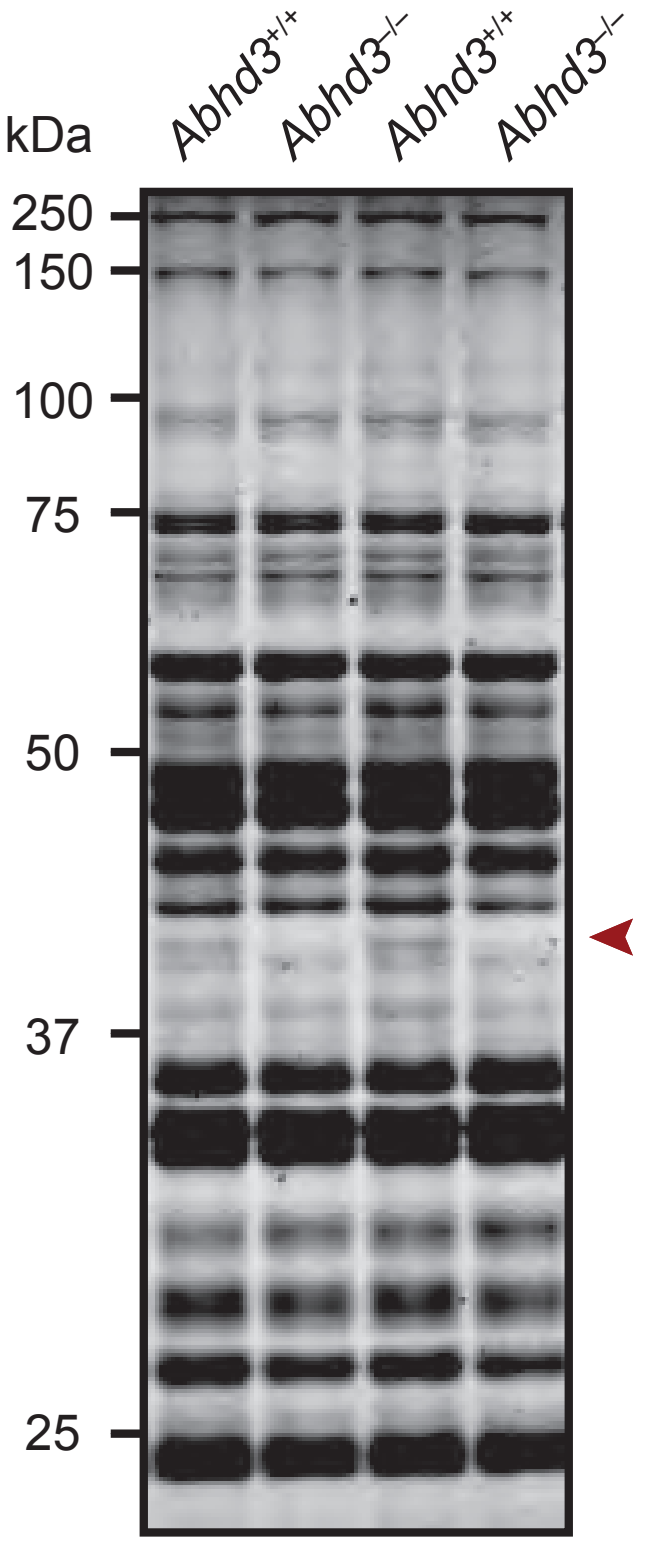

Supplementary Fig. 9

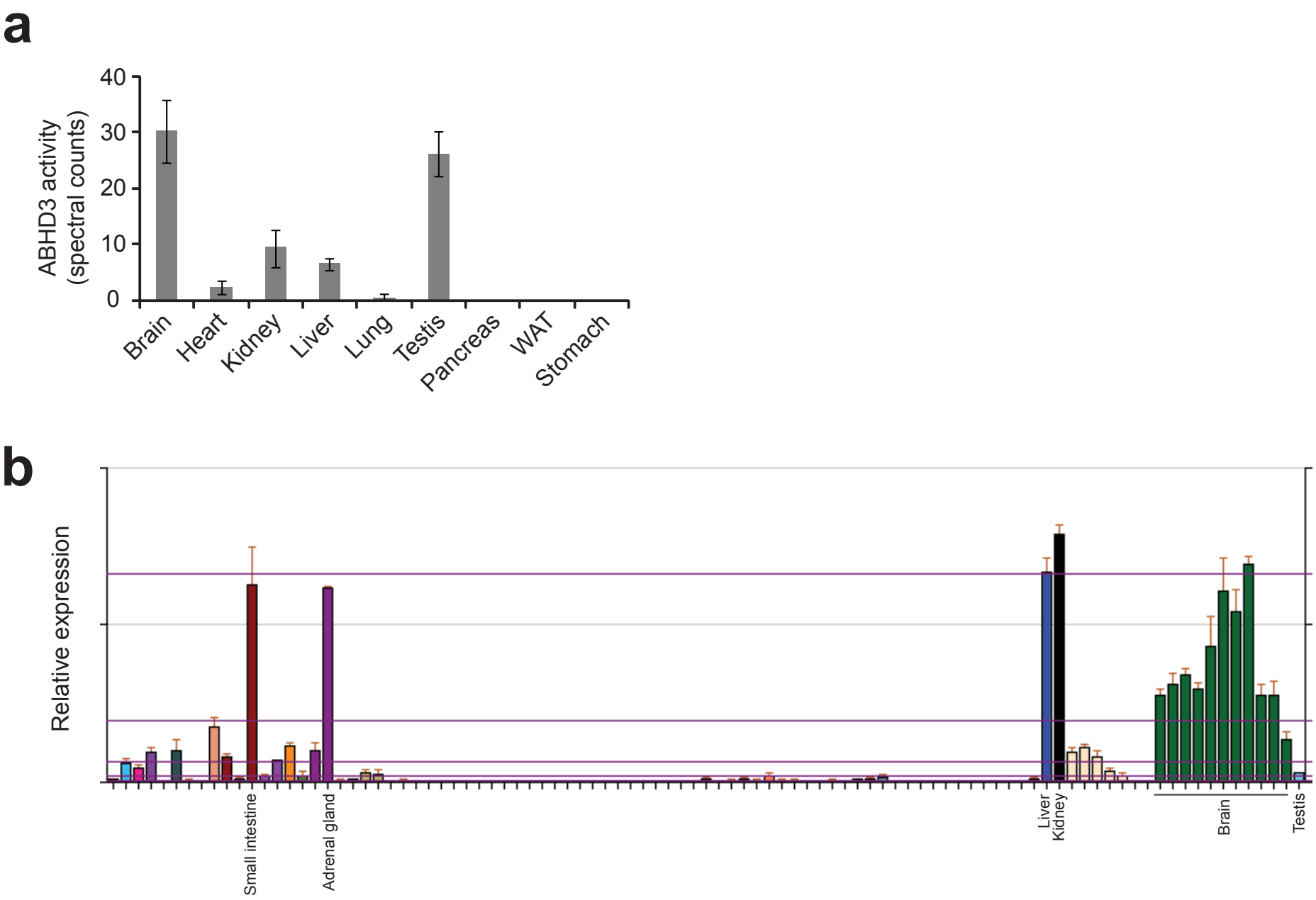

Supplementary Fig. 10

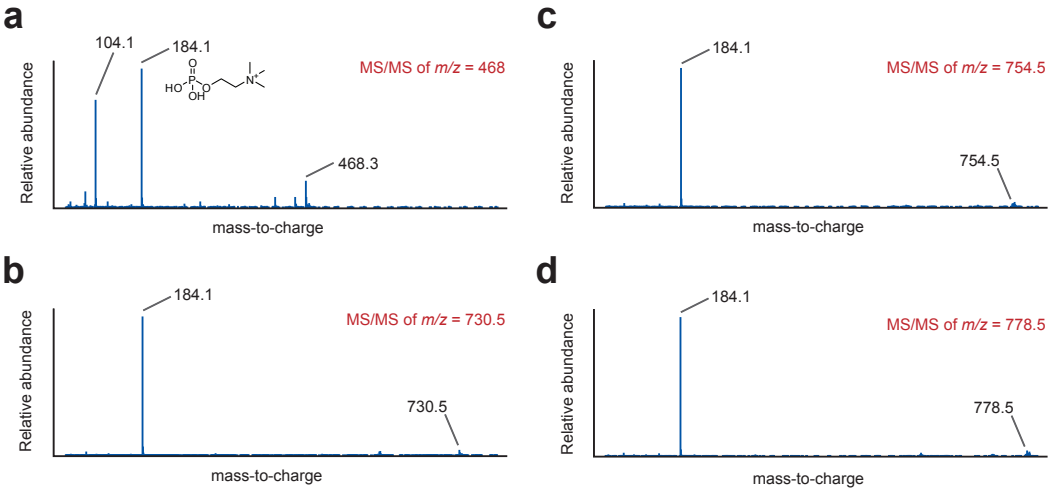

Supplementary Fig. 11

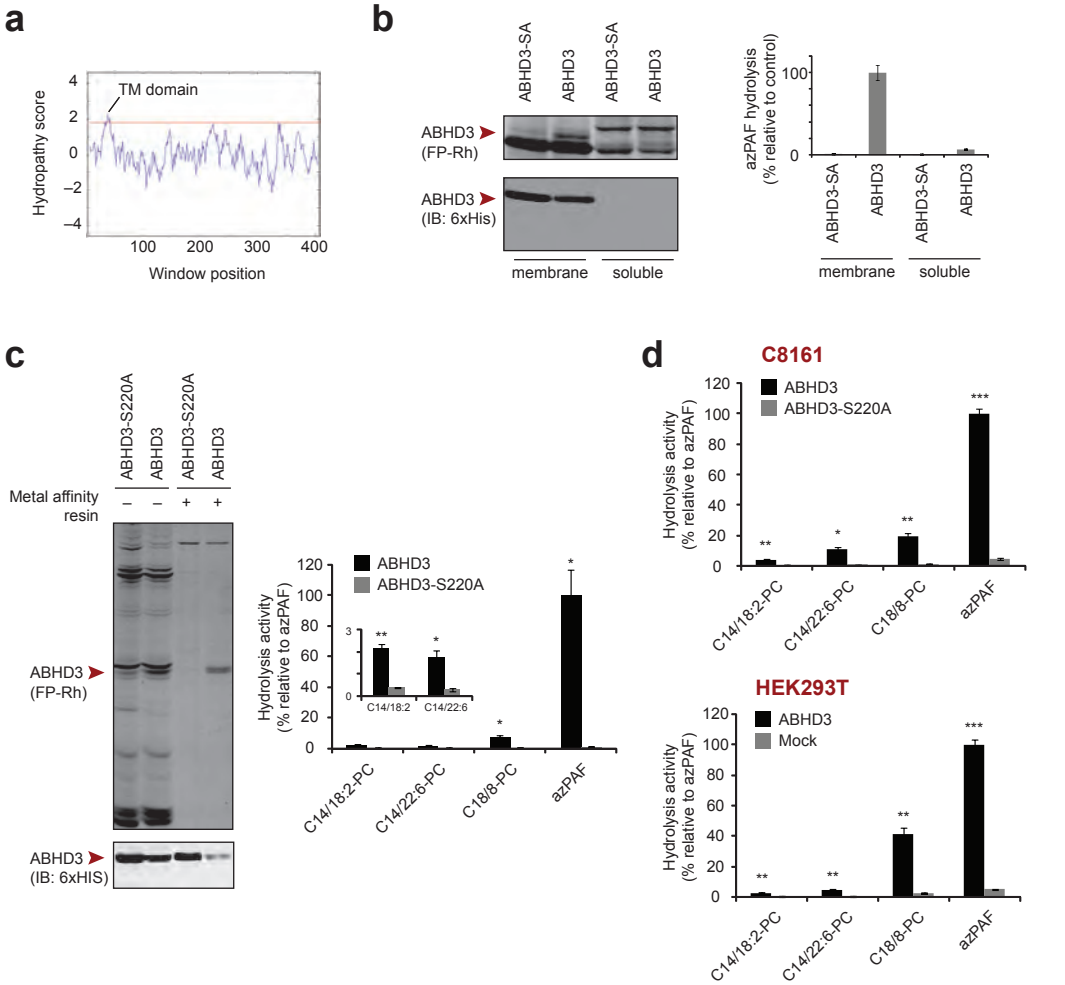

Supplementary Fig. 12

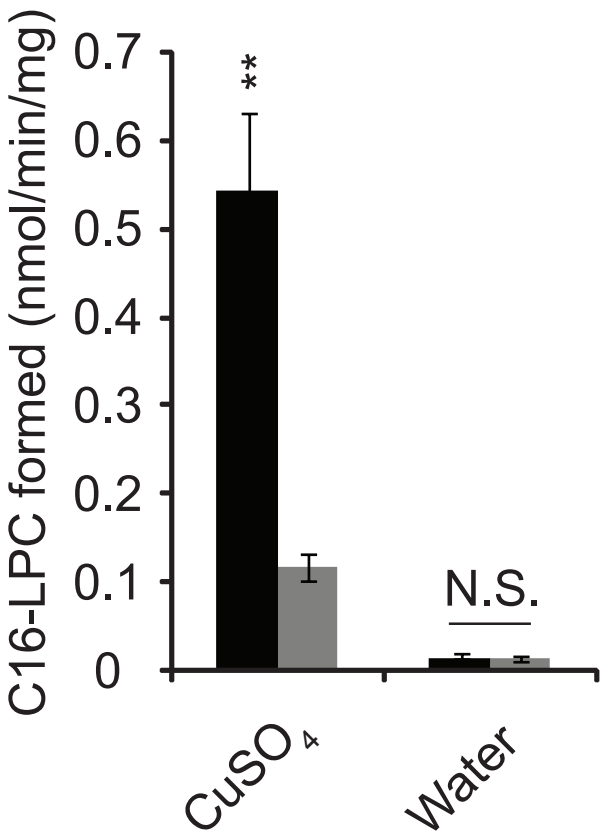

Supplementary Fig. 13